

1 **Dynamical causes of the 2010/11 Texas-northern**
2 **Mexico drought**

3 RICHARD SEAGER *

Lamont Doherty Earth Observatory of Columbia University, Palisades, New York

4 LISA GODDARD

International Research Institute for Climate and Society, Palisades, New York

5 JENNIFER NAKAMURA, NAOMI HENDERSON, DONNA LEE

Lamont Doherty Earth Observatory of Columbia University, Palisades, New York

* *Corresponding author address:* Richard Seager, Lamont Doherty Earth Observatory of Columbia University, 61 Route 9W., Palisades, NY 10964. Email: seager@ldeo.columbia.edu

Submitted to *Journal of Hydrometeorology* January 2013. LDEO Contribution Number xxxx.

ABSTRACT

7 The causes of the Texas-northern Mexico drought during 2010-11 are examined using ob-
8 servations, reanalyses and model simulations. The drought began in fall 2010 and winter
9 2010/11 as a La Niña event developed in the tropical Pacific Ocean. Climate models forced
10 by observed sea surface temperatures (SSTs) produced dry conditions in fall 2010 through
11 spring 2011 strongly influenced by transient eddy moisture flux divergence related to a north-
12 ward shift of the Pacific-North America storm track, typical of La Niña events. In contrast
13 the observed drought was not associated with such a clear shift of the transient eddy fields
14 and instead was significantly influenced by internal atmospheric variability including the
15 negative North Atlantic Oscillation of winter 2010/11 which created mean flow moisture
16 divergence and drying over the southern Plains and southeast. The models suggest that
17 drought continuation into summer 2011 was not strongly SST-forced. Mean flow circulation
18 and moisture divergence anomalies were responsible for the summer 2011 drought, arising
19 from either internal atmospheric variability or a response to dry summer soils not captured
20 by the models. Summer of 2011 was one of the two driest and hottest summers over recent
21 decades but does not represent a clear outlier to the strong inverse relation between summer
22 precipitation and temperature in the region. Seasonal forecasts at 3.5 month lead time did
23 predict onset of the drought in fall and winter 2010/11 but not continuation into summer
24 2011 demonstrating the current, and likely inherent, inability to predict important aspects
25 of North American droughts.

1. Introduction

In the fall of 2010 the U.S. Drought Monitor showed no areas of the U.S. in drought, a situation essentially unique since the Drought Monitor was initiated in 1999 as an easy-to-understand means of tracking drought status. By fall 2010 the southwest drought that began after the 1997/98 El Niño had finally ended and the southeast drought of 2007/8 was long and gone. However, even as the Drought Monitor was showing unusually moist conditions across the country, seasonal-to-interannual forecasts were predicting a return to dry conditions across the southern U.S. and northern Mexico in the winter ahead. Those forecasts were based on forecasts of a developing La Niña in the tropical Pacific Ocean. Historically La Niña events have led to drier than normal conditions in the southwest U.S. northern Mexico, the southern Plains and southeast U.S and wetter than normal conditions in the Pacific northwest (Ropelewski and Halpert 1986; Mason and Goddard 2001; Seager et al. 2005a). This turned out to be a good forecast for much of the southern U.S. in winter 2010/11 which experienced drier than normal conditions except in southern California.

The interior southwestern states of the U.S. receive most of their precipitation in the winter and, hence, this was sufficient to move those states back towards abnormal dryness or drought. In Texas, precipitation is more evenly distributed throughout the year, and the dry winter was followed by a dry spring and a dry summer which, in sum, were sufficient to cause one of the most catastrophic short-term droughts in U.S. history. As is usually the case, dry conditions in the southern Plains went along with higher than normal temperatures and Texas and surrounding regions in summer 2011 broke records for the warmest summer on record. The costs in terms of U.S. agricultural losses were staggering. The National Climatic Data Center estimated it at \$12 billion (<http://www.ncdc.noaa.gov/billions/events.pdf>). The Texas drought, combined with the spring 2011 tornado season, floods in the Mississippi basin and Hurricane Irene, made 2011 the costliest ever in terms of weather and climate related disasters. The vulnerability of the U.S. to extreme weather and climate events has never been so clear. Meanwhile in Mexico in November 2011 the Secretary for Social Development reported that drought had left 2.5 million Mexicans with insufficient drinking water (<http://www.radioformula.com.mx/notas.asp?Idn=210675>) and shortages of basic foodstuffs

55 led to a large increase in imports from the U.S. (<http://www.mnoticias.com.mx/note.cgi?id=403006>).
56 Mexico has been suffering a drought since the mid 1990s (Seager et al. 2009; Stahle et al.
57 2009) so the severity of the 2011 drought further revealed the climatic vulnerability of Mex-
58 ico.

59 This paper focuses on the Texas-northern Mexico (hereafter TexMex) drought and ad-
60 dresses the question of what caused it? This is an important question in that it has been
61 argued that anthropogenic global warming should lead to aridification of the subtropics and
62 a poleward expansion of subtropical dry zones and also a shift to more extreme precipi-
63 tation events. Was the TexMex drought a case of such anthropogenically induced climate
64 change? It would certainly be rash to draw such a conclusion given that past droughts in
65 the southwest and Plains have been reliably attributed to forcing of atmospheric circulation
66 anomalies by naturally occurring cool tropical Pacific and, to a lesser extent, warm tropical
67 North Atlantic sea surface temperature (SST) anomalies (Schubert et al. 2004b,a; Seager
68 et al. 2005b; Herweijer et al. 2006; Seager 2007). This most recent drought also coincided
69 with a La Niña event. Indeed a recent study (Hoerling et al. 2013) has concluded that
70 the summer of 2011 Texas drought and heatwave was within the range of natural variability
71 of the atmosphere-ocean-land surface system, made much more likely by the La Niña of
72 2010/11 and, only to a lesser extent, by anthropogenic climate change.

73 While the 2010/11 drought and heat wave were decidedly severe this event is, by the
74 standards of recent history, so far quite brief. The records that were broken during the event
75 were often set in the 1930s and 1950s during two devastating multiyear droughts created by
76 some mix of tropical Pacific and Atlantic SST variations and internal atmospheric variability
77 and, for the 1930s Dust Bowl drought, dust aerosol forcing (Schubert et al. 2004b,a; Seager
78 et al. 2005b, 2008; Cook et al. 2008, 2009, 2010; Hoerling et al. 2009). By the standards of
79 those droughts, or some 19th Century droughts (Stahle and Cleaveland 1988; Herweijer et al.
80 2006), the 2010/11 drought was intense but brief. However, after a relatively wet winter in
81 2011/12, especially in eastern Texas, at the time of writing (September 2012) the Drought
82 Monitor shows extreme to exceptional drought in the central Plains and dry conditions to
83 severe drought extending across most of Texas, the southwest, the Rockies and the midwest
84 so this event is not yet over.

85 In this paper we focus on the dynamical causes of the 2010/11 TexMex drought in terms of
86 circulation anomalies and variations of surface evaporation and transports and convergence
87 of moisture within the atmosphere and examine its evolution from fall of 2010 to its most
88 extreme state in summer and fall of 2011. Our goal is to determine the ocean-atmosphere
89 dynamics of this event and, by reference to prior work, assess how similar or different it
90 was to other droughts in the region and the typical seasonal-to-interannual variability of
91 hydroclimate in the region forced by the tropical oceans. As part of this effort we will examine
92 how well the drought can be reproduced in atmosphere models forced by the observed SSTs
93 and, hence, the potential predictability of the event. In addition we will examine how well
94 the event was actually forecast in advance which depended on the ability to forecast the
95 SSTs and the atmospheric response to them and any atmospheric response to prior land
96 surface conditions.

97 A comprehensive analysis and understanding of the 2010/11 TexMex drought, and its
98 predictability, will inform decision making and disaster planning by allowing assessment of
99 its likelihood, advance warning signs and ability to predict ahead of time, or lack thereof.
100 This will also inform attempts to assess whether this event arose from natural variability,
101 and akin to prior events, or bore an imprint of anthropogenic climate change which, in turn,
102 influences likelihood of similar events in the future.

103 **2. Observational and model data**

104 The observed precipitation data is from the National Oceanic and Atmospheric Adminis-
105 tration/National Centers for Environmental Prediction (NCEP) Climate Prediction Center
106 (Chen et al. 2002) available from the Data Library of the International Research Institute for
107 Climate and Society (<http://iridl.ldeo.columbia.edu>) and which cover 1948 to present. For
108 the analyses of observed SST, atmospheric circulation and surface air temperature we use
109 data from the NCEP/National Center for Atmospheric Research (NCEP/NCAR) Reanalysis
110 covering 1949 to present (Kalnay et al. 1996; Kistler et al. 2001).

111 The first model used is the NCAR Community Climate Model 3 (CCM3, which has been
112 used extensively by us for North American drought research (e.g. Seager et al. (2005b)).

113 NCAR has released many atmosphere models since CCM3 and all have been experimented
114 with at Lamont Doherty Earth Observatory but none found to be as skillful at reproducing
115 the observed history of U.S. southwest and Plains precipitation as CCM3. Hence, despite
116 its vintage, we use CCM3 here. The model is forced by observed SSTs which are from the
117 Kaplan et al. (1998) data in the tropical Pacific Ocean and the Hadley Centre data (Rayner
118 et al. 2003) elsewhere. 16 ensemble members were generated with different initial conditions
119 and results are primarily shown for the ensemble mean, which averages over uncorrelated
120 weather in the members and closely isolates the common SST-forced component. The simu-
121 lations begin on January 1 1856. Unlike in Seager et al. (2005b), the simulations here also
122 have the observed increases in CO_2 and CH_4 imposed allowing land surfaces to warm and
123 the atmospheric circulation to adjust to the changes in radiative properties. The other model
124 is the European Centre-Hamburg 4.5 (ECHAM4.5, Roeckner et al. (1996) and we use a 24
125 member ensemble from 1950 on available in the International Research Institute for Climate
126 and Society Data Library (<http://iridl.ldeo.columbia.edu/docfind/databrief/cat-sim.html>).

127 We also use the NCEP-NCAR reanalysis and the European Centers for Medium Range
128 Weather Forecasts (ECMWF) Reanalysis-Interim (ERA-I, Dee et al. (2011)) data sets to
129 evaluate the components of the moisture budget that caused precipitation anomalies during
130 the drought. For both reanalyses we evaluate anomalies of the convergence or divergence
131 of the vertically integrated moisture transports by (i) the mean flow and (ii) the transient
132 flow. The former is evaluated using monthly mean values of winds and specific humidity
133 and the latter using co-variances of departures of the daily values from the monthly means.
134 The vertical integrals extend to the monthly mean surface pressure. It should be noted
135 that evaluating the moisture budget in this way diagnostically from Reanalysis data leads
136 to significant errors compared to the actual moisture budget calculation in the models that
137 produce the Reanalyses due to differences in the numerical methods used and the time
138 resolution of the calculation. This is the topic of another paper (Seager and Henderson
139 2013) where it is shown that, if care is taken to adopt the best computational methods, as
140 is the case here, diagnostic evaluation of moisture budget components can produce useful
141 results.

142 Anomalies shown here are computed relative to the period that is common to all the

143 models and observations, January 1950 to November 2011. The only exception is for the
144 ERA-I which begins in 1979 and for which we assess anomalies relative to a 1979 to 2011
145 climatology.

146 **3. Typical La Niña associated precipitation and circu-** 147 **lation anomalies in the Pacific-North America**

148 Since the 2010/11 drought was associated with full and then waning La Niña conditions
149 we first of all review the typical precipitation and circulation anomalies in the Pacific-North
150 America region associated with La Niñas for later comparison with what happened during
151 the 2010/11 event. This was done based on the NINO3 index (SST anomalies averaged
152 over $5^{\circ}S - 5^{\circ}N, 130^{\circ} - 90^{\circ}W$) which was formed into DJF, MAM, JJA and SON seasonal
153 anomalies. The years when the anomaly values were less than one standard deviation were
154 then identified. Values of observed SST, and observed and modeled precipitation and 200mb
155 height, were then composited for these years to provide seasonal values of typical La Niña
156 conditions¹.

157 *a. Observed canonical La Niña conditions*

158 SST anomalies are well developed in SON and go along with a high anomaly over the
159 mid-latitude west Pacific and North America and dry anomalies across the U.S. and Mexico
160 from southern California to the Atlantic (Figure 1). The classic ENSO pattern is clear in
161 DJF with a cyclonic anomaly immediately north of the cold tropical Pacific SST anomaly, a
162 well developed North Pacific high anomaly that merges with a zonal band of high pressure
163 over North America and the mid-latitude Atlantic Ocean. Dry conditions extend across

¹The years and seasons identified as La Niñas were 1950 (MAM, JJA, SON), 1955 (SON), 1956 (JJA),
1964 (JJA, SON), 1970 (JJA, SON), 1971 (MAM, JJA, DJF), 1973 (JJA, SON), 1974 (MAM, JJA, DJF),
1975 (MAM, JJA, SON), 1976 (MAM, DJF), 1985 (DJF), 1988 (JJA, SON), 1989 (MAM, DJF), 1999
(all seasons), 2000 (MAM, DJF), 2007 (SON), 2008 (MAM, DJF), 2010 (JJA, SON), 2011 (MAM, DJF)
where DJF 2011 indicates DJF 2010/11 for example. The two models used different SST data sets and, in
particular, have some additional La Niña seasons in 1954, 1955 and 1956.

164 Mexico and the southern portions of the U.S. with a maximum at the Gulf coast. La Niña
165 SST anomalies are typically weaker in MAM and so are the circulation and precipitation
166 anomalies. Even though the SST anomalies remain in JJA, the circulation anomalies are
167 weak, consistent with our understanding of the seasonal cycle of tropical to mid-latitude
168 teleconnections.

169 *b. Modeled canonical La Niña conditions*

170 The models use different SST data sets to that used for the SST anomalies shown in
171 Figure 1 but the differences are very small. CCM3 shows a typical La Niña height response
172 from SON through MAM with a ridge extending from the North Pacific to the mid-latitude
173 Atlantic with a localized high somewhere over North America in each season (Figure 2).
174 This is also the case for ECHAM4.5 (Figure 3) but with the SON anomalies weaker, and
175 the DJF anomalies stronger, than in CCM3. The SON La Niña precipitation anomalies
176 in both models show wet in the Pacific northwest and dry across most of the rest of the
177 continent as observed (Figure 1). The observed north-south wet-dry La Niña dipole in DJF
178 is best modeled by ECHAM4.5 while CCM3 continues with the wet Pacific northwest and dry
179 everywhere else pattern seen in SON. CCM3 produces widespread dry anomalies in MAM
180 and JJA of La Niñas in contrast to the more spatially variable observed La Niña precipitation
181 anomalies in these seasons. ECHAM4.5 produces MAM precipitation anomalies that are far
182 too strong but have some of the observed pattern with dry conditions in the southwest.
183 ECHAM4.5 also produces far too extensive dry conditions over the U.S. and Canada in La
184 Niña JJAs but does capture the wet conditions in Mexico and Central America.

185 **4. SSTs during the 2010/11 TexMex drought**

186 Returning to the specific case of 2010/11, Figure 4 shows the history of sea surface
187 temperature and surface air temperature over land during the drought. In fall (September
188 to November, SON) of 2010 a strong La Niña had already developed with anomalies of
189 around -2°C while the tropical Atlantic Ocean was warmer than normal. The La Niña

190 was still strong in winter (December to February, DJF) 2010/11 and the SST anomalies in
191 both oceans then weakened through spring (March to May, MAM) and summer (June to
192 August, JJA) of 2011. By summer of 2011 the La Niña was essentially gone and the tropical
193 Atlantic SST anomalies were also weak. The La Niña began to reform in fall of 2011 (and
194 developed into another La Niña for winter 2011/12, not shown). Temperatures over North
195 America were actually colder than normal in winter 2010/11, especially in the eastern U.S.
196 Anomalous heat developed in Mexico, the southern and central Plains and the southeast in
197 spring 2011 and maximized in the summer with a bulls eye centered on the central Plains
198 and extending over northern Mexico and the entire eastern U.S. The fall 2010 and winter
199 2010/11 SST pattern would be expected to force dry conditions across the southern U.S.
200 both as a response to the cold tropical Pacific SSTs and the warm tropical North Atlantic
201 SSTs, an ideal configuration for forcing North American drought (Schubert et al. 2009).
202 However the continuation and intensity of the drought in summer and fall 2011 is hard
203 to reconcile with contemporaneous SST forcing since the SST anomalies are weak by that
204 season. This suggests a role for either land surface feedback that can extend the drought
205 forward in time after being initiated by prior SST forcing or a role for random internal
206 atmospheric variability. Tropical Pacific SST anomalies are known to be quite predictable
207 on the seasonal-to-interannual timescale (e.g. Jin et al. (2008)) so it would also be expected
208 that the component of the drought forced from the tropical Pacific could be predicted several
209 months ahead of time.

210 **5. Comparison of observed and model-simulated pre-** 211 **cipitation anomalies during the TexMex drought**

212 Figure 5 shows for 3 months seasons beginning in September to November 2010 and
213 ending in September to November 2011 the observed precipitation anomalies and those
214 modeled by the CCM3 and ECHAM4.5 models when forced by the observed SSTs. The
215 actual precipitation anomaly was consistently negative across Texas and Mexico and much
216 of the surrounding states throughout this entire 15 month period. Dry anomalies were

217 modest in fall 2010 but were in full force in DJF 2010/11 and centered in the southeast,
218 strong and centered in Mexico and the south-central U.S. in MAM 2011 and then intensified
219 and spread into JJA 2011 and persisted into SON 2011. In JJA and SON 2011 the drought
220 was very centered on Texas and northern Mexico although, in fall, most of the west and
221 central U.S. was also dry while the midwest and northeast were very wet. From SON 2010
222 to MAM 2011 the observed precipitation anomalies have some similarity with those typical
223 for La Niña conditions during those seasons (Figure 2) but the strong summer drying is not
224 typical.

225 The models simulate widespread dry conditions across most of the U.S. and Mexico in fall
226 2010 and the southern U.S. and Mexico in winter 2010/11. These model patterns are quite
227 similar to those observed except over California where the models simulated dry conditions as
228 a typical model La Niña response (Figures 3 and 4) but, in fact, atypically a wet fall 2010 and
229 winter 2010/11 actually occurred. In MAM 2011 the models simulate dry conditions across
230 most (CCM3) or all (ECHAM4.5) of Mexico and almost all of the U.S. and fail to reproduce
231 the north-south wet-dry dipole actually observed, although ECHAM4.5 does simulate the
232 wet midwest and northeast observed. The model precipitation anomalies in MAM 2011 are
233 similar to their canonical La Niña responses. After spring, as the La Niña faded away, the
234 models generally fail to reproduce the focused and strong northern Mexico-Texas drought
235 in summer and fall 2011 although ECHAM4.5 does produce widespread but modest drying
236 across the U.S. and northern Mexico. Hoerling et al. (2013) show results for June through
237 August for SST forcing of the atmosphere model component of the National Atmospheric
238 and Oceanic Administration’s Climate Forecast System version 2. That model also produces
239 drying that is only half as strong as that observed and also not focused in the TexMex area.
240 The results from these models indicate that the beginning of the drought in fall 2010 and
241 winter 2010/11 was related to the development of SST anomalies but that the intensity of
242 the drought in summer and fall 2011 was not uniquely a response to SST anomalies and
243 hence must have had other causes.

244 Table 1 lists the area-weighted anomaly correlation coefficients between observed and
245 modeled precipitation anomalies for land areas between $20^{\circ}N$ and $50^{\circ}N$ providing a quanti-
246 tative measure to go with the description above. ECHAM4.5 performs better than CCM3,

247 especially in MAM and JJA 2001, the models are very similar in the DJF 2010/11 precipita-
248 tion patterns and both have similarity to the observed pattern (all reflecting similar patterns
249 of response to SST forcing) and the models fail to reproduce the observed pattern in SON
250 2011.

251 **6. Causes of the 2010/11 TexMex drought: modeled** 252 **and reanalyzed moisture budget anomalies**

253 *a. Modeled moisture budget anomalies*

254 The two atmosphere models used here, together with the two Reanalyses, provide some
255 indication of the causes of the drought and hence we analyze the variations in the atmo-
256 spheric branch of the hydrological cycle within the models to determine how changes in
257 evaporation and moisture convergence by the mean and transient flow combined to generate
258 lower than normal precipitation. Figures 6 through 10 show anomalies in modeled precipi-
259 tation, evaporation and convergence of vertically integrated moisture transport by the mean
260 flow and by transient eddies for the seasons from fall 2010 through fall 2011.

261 In SON 2010 (Figure 6) the reduction of precipitation simulated by both the CCM3 and
262 ECHAM4.5 models is sustained by a spatially varying mix of a reduction of evaporation,
263 mean flow moisture convergence and transient eddy moisture convergence. Both models
264 agree that the transient eddy moisture convergence anomaly at this time is not very orga-
265 nized. Also, both models agree that the mean flow moisture convergence anomaly moistens
266 the Pacific coast states of the U.S. and Baja California and provides broad areas of drying
267 over the central and eastern U.S. and parts of Mexico.

268 In DJF 2010/11 (Figure 7) the models agree that the negative precipitation anomaly
269 focuses across the southern U.S. and all of Mexico with negative evaporation anomalies
270 in roughly the same area. Most impressive is that the models agree that there is a strong
271 region of anomalous transient eddy moisture *divergence* stretching from northern Mexico and
272 Texas across the entire eastern U.S. while the mean flow produces a moisture convergence
273 anomaly in roughly the same area but dries western Texas and the interior southwest U.S.

274 The same drying of northern Mexico, Texas and the eastern U.S. by anomalous transient
275 eddy moisture flux divergence occurs in both models in MAM 2011 while anomalous mean
276 flow moisture divergence causes widespread drying across the central and northern Plains,
277 Rocky Mountains and Great Lakes region (Figure 8).

278 In JJA 2011 (Figure 9) only ECHAM4.5 has a strong negative precipitation anomaly
279 across the U.S. and Mexico. In this season the transient eddy moisture flux anomalies are
280 weak and, in ECHAM4.5, the mean flow moisture convergence creates a dry anomaly across
281 northwestern Mexico, the southwest, the Pacific coast states and the Rockies. Both models
282 have widespread negative evaporation anomalies indicative of dried soils. In SON 2011
283 (Figure 10) the precipitation anomalies are amorphous in CCM3 but remain widespread and
284 negative in ECHAM4.5 and are coincident with reduced evaporation. Both models agree
285 on a renewed drying tendency by transient eddy moisture flux divergence in the central
286 U.S. including Texas while ECHAM4.5 still has a mean flow moisture divergence anomaly
287 creating a drying tendency in northern Mexico, the southwest and Rocky Mountains.

288 *b. Moisture budget anomalies in the NCEP-NCAR and ERA-I reanalyses*

289 By virtue of ensemble averaging, the variations in moisture convergence or divergence in
290 the models are caused by changes in the mean and transient atmospheric circulation that
291 are forced by the imposed SSTs. These variations can be contrasted with those that actually
292 occurred, as realized in Reanalyses, to assess the realism of the SST-forced variations and
293 their importance relative to variations associated with internal atmospheric variability not
294 associated with particular ocean conditions. In Figure 11 we show the history of variations
295 in the convergence and divergence of vertically integrated moisture transport by the mean
296 flow and the transient circulation as diagnosed from the NCEP-NCAR Reanalysis. In the
297 first two seasons of the drought (SON 2010 and DJF 2010/11) the NCEP-NCAR Reanalysis
298 indicates that it is anomalous moisture divergence by transient eddies that contributes a
299 drying trend across the southern U.S. in fall and the central U.S. in winter. In MAM 2011
300 the NCEP-NCAR moisture budget has only a transient eddy moisture divergence anomaly
301 causing drying over southern, mid-Atlantic and northeastern states. In JJA and SON 2011

302 mean flow moisture divergence anomalies do cause extensive drying in the drought region.

303 The NCEP-NCAR moisture divergence anomalies bear some resemblance to the observed
304 precipitation anomalies (Figure 5, the drying tendency in the Plains and wetting tendency in
305 the northeast in SON 2011 particularly closely matches the observed precipitation pattern).
306 However the differences are also sufficiently large that it makes sense to examine the ERA-I
307 Reanalysis as well (Figure 12). The ERA-I Reanalysis reports the divergence of the vertically
308 integrated moisture transport as a diagnostic quantity which is presumably evaluated on the
309 model grid and at the model time step and, hence, is close to that actually evaluated during
310 the model analysis cycle. This is plotted along with the mean and transient flow components
311 as computed by us. With the partial exception of MAM and JJA 2011, the actual ERA-I
312 Reanalysis moisture divergence or convergence anomaly quite closely matches the observed
313 precipitation anomaly. Since the sum of the two components quite closely matches the actual
314 divergence or convergence (not shown) the partition can be considered valid and useful.

315 Comparing Figures 11 and 12, it is seen that there is notable agreement between the
316 two Reanalyses in the patterns of moisture divergence and convergence by the mean and
317 transient flow. ERA-I suggests a mean flow drying of Texas and the Plains in SON 2011
318 in addition to the transient flow drying of much of southern North America which NCEP-
319 NCAR and ERA-I agree upon. In DJF 2011 ERA-I also suggests a mean flow moisture
320 divergence anomaly drying Texas, northeast Mexico and the southeast adding to a more
321 general transient component drying that again agrees with NCEP-NCAR. In MAM 2011
322 ERA-I agrees with NCEP-NCAR with a transient component drying from northeast Mexico
323 to the northeast that is opposed by a mean flow moistening. In JJA 2011, at the height
324 of the 2010/11 drought, ERA-I indicates that anomalous mean flow moisture divergence
325 was widespread across North America, largely confirming the results from NCEP-NCAR.
326 Widespread, but weaker, mean flow moisture convergence anomalies persisted into SON
327 2011, again confirming the NCEP-NCAR results.

328 In summary, both Reanalyses suggest that the drought was caused by a combination of
329 mean and transient flow moisture divergence anomalies in fall 2010 and winter 2010/11 but
330 that by spring, summer and fall 2011 the mean flow divergence anomalies were dominant.
331 The next step is to relate these anomalies in the moisture budget to the anomalies in the

332 mean and transient atmospheric circulation.

333 **7. Causes of the 2010/11 TexMex drought**

334 *a. Mean atmospheric circulation anomalies*

335 In relating the moisture convergence and divergence anomalies to circulation anomalies
336 we make use of the simple concept that increased moisture convergence and precipitation
337 are associated with rising motion and vice versa, as shown for El Niño and La Niña in prior
338 work (Seager et al. 2005a). Then we expect, on large scales, rising motion anomalies to
339 be found where the mean flow is poleward, and descending motion where the mean flow is
340 equatorward, according to a simple vorticity balance between advection of planetary vorac-
341 ity and vortex stretching and thermal balance between meridional advection and adiabatic
342 cooling or warming due to vertical motion and expansion or compression. Of course the
343 vorticity and thermal budgets controlling the location of vertical motion anomalies are in
344 reality more complex than this but this reasoning will be applied below to guide the linking
345 of circulation and moisture budget anomalies.

346 In Figure 13 we show the Reanalysis 200mb height anomalies by season from SON 2010
347 through SON 2011 together with the ensemble mean of the CCM3 and ECHAM4.5 sim-
348 ulations. In SON 2010 the observations show mid-latitude high pressure over Asia and
349 the western North Pacific, a low over the Pacific northwest, a high over the central North
350 America and a low over the eastern seaboard and western North Atlantic. This is quite
351 similar to the typical fall La Niña height anomaly pattern (Figure 5). This height pattern is
352 consistent with increased precipitation in the northwest U.S. and western Canada and dry
353 anomalies further south as observed (Figure 5) with mean flow moisture convergence and
354 divergence anomalies being responsible (Figure 11 and 12). Low height anomalies over the
355 tropical Pacific are forced by the cold La Niña SST anomalies. Consistent with that, the two
356 models also show negative height anomalies over the tropical Pacific with the characteristic
357 off-equatorial cyclones. The models also have widespread subtropical to mid-latitude ridges
358 characteristic of La Niña (Seager et al. 2003) with high anomalies over the North Pacific

359 and southern North America, again typical of the response to La Niña forcing (e.g. Strauss
360 and Shukla (2002)). The two models' height anomalies are very similar to each other and
361 provide evidence that the subtropical to mid-latitude highs over Asia, the North Pacific and
362 North America were largely a forced response to the emerging 2010/11 La Niña. The low
363 anomaly west of Canada and the anomalies over the North Atlantic are not reproduced in
364 the SST-forced models but are in the observed SON La Niña composites suggesting that the
365 models are not capable of simulating these features faithfully (as seen in Figures 1 to 3).

366 In DJF 2010/11 the reanalysis shows the development of a strong high over the North
367 Pacific that extends into western North America. This is a typical La Niña-forced pattern
368 (Figure 1) but similarity is not seen over eastern North America and the Atlantic where a
369 strong negative North Atlantic Oscillation (NAO) event developed. The reanalysis observa-
370 tions also show strong low height anomalies over the tropical Pacific Ocean consistent with
371 forcing from the underlying cold La Niña SST anomalies. Both SST-forced models show
372 the low heights over the tropical Pacific, though weaker than those observed. ECHAM4.5
373 also develops a strong high over the North Pacific, albeit east of the observed one while,
374 oddly, the CCM3 has only weak and poorly defined high anomalies over the North Pacific.
375 The models, not surprisingly, fail to produce the negative NAO event and the ECHAM4.5
376 simulation is, instead, quite reminiscent of a typical La Niña pattern. The observed height
377 anomalies, including the contribution of the NAO in generating strong northerly flow over
378 the central and eastern U.S., are consistent with negative precipitation anomalies in the
379 southwest U.S. and across the central and eastern southern U.S. as observed (Figure 5) with
380 anomalous mean flow moisture divergence responsible (Figures 8 and 9). In contrast, the
381 ECHAM4.5 height anomalies would be expected to cause reduced precipitation over the west
382 coast of North America due to anomalous mean flow moisture divergence. The modeled high
383 off the U.S. southeast is consistent with modeled anomalous mean flow moisture divergence
384 to its east (over the Atlantic) and anomalous mean flow moisture convergence to its west
385 over the eastern U.S. (Figure 7) which is distinct from the observed NAO-induced drying in
386 the region.

387 In MAM 2011 the models retain the same character of a La Niña forced height anomaly
388 pattern both in the tropics and extratropics as they showed in the previous season consistent

389 with the continued, but weakening, cool tropical Pacific SSTs. In the reanalysis observa-
390 tions the low anomalies over the tropical Pacific are also present but there was a band of
391 low pressure stretching from Korea to western Canada with similarly zonally oriented high
392 anomalies sandwiched between here and the tropical low anomalies. This has some similarity
393 to the observed MAM La Niña composite (Figure 1) and, as for SON 2010, the observations
394 seem to combine a forced response to the waning La Niña with a substantial component
395 of internal atmospheric variability. The observed height anomalies drive westerly anomalies
396 into the Pacific Northwest consistent with a wet Pacific Northwest and drier conditions to
397 the south as observed (Figure 5) with mean flow moisture convergence/divergence anomalies
398 the cause. The model precipitation anomalies, with dry anomalies extending further north
399 than observed (Figure 5), and drying by a combination of mean flow moisture divergence (to
400 the north) and transient eddy moisture divergence (to the south) (Figure 8), are different to
401 observations but consistent with their more canonical La Niña height anomalies.

402 In JJA 2011, as the La Niña continued to wane, the models provide no evidence of a
403 strong extratropical circulation response with only weak positive height anomalies over North
404 America. The reanalysis observations however show a localized upper level high anomaly,
405 and low level low (not shown), over the North American continent (quite unlike the very
406 weak composite JJA La Niña pattern in Figure 1). The JJA 2011 patterns are consistent
407 with the precipitation anomalies: the observations show a strong dry anomaly under the
408 high anomaly and the models have much weaker and more amorphous dry anomalies. The
409 suggestion is that the JJA 2011 dry anomaly was a result of either internal atmospheric
410 variability, rather than ocean forcing, or a forced response to dry soils that was not captured
411 by the models. In SON 2011 the La Niña regained strength, and this time the CCM3 model
412 responded with a canonical height anomaly while ECHAM4.5 did not. The observed height
413 anomaly appears dominated by internal atmospheric variability and has a high over northeast
414 Canada and a low over the southern U.S and western Canada. This favored dry conditions
415 over much of the southern U.S. and wet conditions over the northeast U.S. via mean flow
416 moisture divergence/convergence anomalies (Figure 5, 11 and 12). The models notably fail
417 to simulate that precipitation pattern consistent with it not being forced by SSTs.

418 In summary, the evolution of the height anomalies in the observations and SST-forced

419 models suggest that the 2010/11 La Niña played an important role in causing the develop-
420 ment of the TexMex drought from fall 2010 to spring 2011 but that even within that season,
421 and entirely for summer and fall of 2011, internal atmospheric variability unrelated to ocean
422 conditions, played a critical role in determining the severity and persistence of the drought.

423 *b. Transient atmospheric circulation anomalies*

424 The previous section attempted to draw connections between changes in precipitation
425 during the 2010/11 TexMex drought and changes in the mean flow, but it was clear from
426 Section 3 that the drought was also caused in some seasons by reduced moisture convergence,
427 or enhanced divergence, by transient eddies. Here we examine the changes in the reanalysis
428 observed and modeled transient eddy fields to attempt to link them to the changes in eddy
429 moisture convergence. As shown in Figure 14, in SON 2010, amidst considerable differences,
430 the reanalysis observations and models agree on a band of increased upper tropospheric
431 eddy meridional velocity variance, $\overline{v'^2}$, that extends across central North America at about
432 40–50°N. The models have a band of reduced variance south of this suggestive of a poleward
433 shift of the storm track as is typical of La Niña events (see (Seager et al. 2010)). If such
434 bands co-locate with bands of increased and decreased poleward eddy moisture transport
435 this would be expected to contribute a transient eddy drying tendency to most of the U.S.
436 in rough agreement with the computed model transient eddy moisture flux convergence
437 anomalies in Figure 6 and the Reanalysis ones in Figures 11 and 12.

438 In DJF 2010/11 the reanalysis observations and models agree on increases in $\overline{v'^2}$ over the
439 North Pacific north of 30 – 40°N and over the Pacific coast of North America. There is
440 little agreement between models and observations further east over North America with the
441 observations showing indistinct features over Mexico and the U.S. and the models showing
442 reduced $\overline{v'^2}$ over Mexico and the southern U.S. and, in ECHAM4.5, increased $\overline{v'^2}$ over the
443 central U.S. In the models the transient eddy anomalies are consistent with a transient eddy
444 moisture divergence (convergence) anomaly over the south and southeastern U.S. (Gulf of
445 Mexico and subtropical Atlantic) and translating into a drying tendency over the land as
446 seen in Figure 7. The disagreement with the observed $\overline{v'^2}$ anomalies suggests that the actual

447 P reduction in this region was not sustained in this way and it could instead have been
448 caused by mean flow moisture divergence associated with the negative NAO event (Figure
449 13).

450 In MAM 2012 the models again agree on strengthening of $\overline{v'^2}$ across the North Pacific
451 and North America on the poleward flanks of the upper tropospheric high anomalies seen in
452 Figure 13 and, once more, this is consistent with a drying tendency due to a transient eddy
453 divergence anomaly to the south (Figure 8). The reanalysis observations have quite different
454 patterns of $\overline{v'^2}$ over the North Pacific but have some similarity to the models with increased
455 $\overline{v'^2}$ over central North America but with the addition of a strong and widespread reduction
456 over Canada. The observed and modeled patterns are consistent with anomalous transient
457 eddy moisture divergence and drying over south central and southeast North America. The
458 transient eddy anomalies are weak in JJA 2011 and, in SON 2011, the observations have
459 increased $\overline{v'^2}$ over North America. Only CCM3 of the two models is roughly consistent with
460 the SON 2011 $\overline{v'^2}$ pattern and has transient eddy drying over the southern U.S (Figure 10)
461 although the reanalyses do not support this (Figures 11 and 12). ECHAM4.5 has a pattern
462 of $\overline{v'^2}$ over the North Pacific and west coast of North America that is similar to that of CCM3
463 but the patterns are quite different over central and eastern North America.

464 In summary, while the reanalysis observed transient eddy anomaly field and transient
465 eddy moisture transports provide some evidence for involvement in generating the drought,
466 especially transient eddy drying over the southern U.S. in MAM 2011, the evidence for
467 SST-forcing of these anomalies, in the sense of agreement between observed and SST-forced
468 ensemble mean patterns, is limited. This probably reflects the mix in observations at the
469 seasonal timescale and for an individual event of a modest SST-forced component with a
470 much larger component of internal atmospheric variability.

471 **8. How unusual was the 2010/11 TexMex drought?**

472 Droughts and heat waves are recurring features of the climate of Texas and Mexico so the
473 question arises as to whether the 2010/11 event was in any way unusual? In the summer of
474 2011 many high temperature records were broken across the region so we focus on the June

475 through August (JJA) season. Figure 15 shows a scatter plot of observed and modeled JJA
476 surface air temperature and precipitation anomalies for the 1950 to 2011 period averaged
477 over land areas between $22^{\circ}N$ and $40^{\circ}N$ and $105^{\circ}W$ and $90^{\circ}W$. The observations show
478 a striking inverse and linear relationship between summer temperature and precipitation
479 with dry conditions going along with high temperatures. This is a simple result of reduced
480 moisture availability at the surface necessitating incoming solar radiation be balanced less
481 by evapotranspiration and more by sensible heat flux and long wave radiative cooling which
482 requires higher surface temperatures. JJA 2011 is marked and stands out as both the driest
483 and hottest JJA since 1950 in this region. However JJA 2011 does not appear as an outlier
484 in that, given the precipitation reduction, the temperature is what would be expected and
485 it is accompanied by a close analog (which is JJA 1980).

486 The values plotted for the two models are from the individual ensemble members and
487 hence, like the observations, contain the effects of both SST-forcing and internal atmospheric
488 variability. The models also produce an inverse relation between temperature and precipita-
489 tion variability comparable in strength to that observed. The individual ensemble member
490 simulations of JJA 2011 are plotted as green crosses and are clearly biased warm for the
491 associated precipitation anomaly. Note that the circles in Figure 15 are color coded accord-
492 ing to year and that for the models the later years are typically warmer than the earlier
493 years. This, and the 2011 values, indicate the effect of global warming which is included in
494 both models via the imposed SST history and additionally in CCM3 via imposed changes
495 in CO_2 and CH_4 . No warming tendency appears in the observations where precipitation is
496 instead the dominant control on JJA temperature. The JJA 2011 precipitation anomalies in
497 CCM3 were scattered around zero (see Figure 5) but were biased dry for ECHAM4.5, some
498 extremely so. Two ensemble members (one from each model) achieved a JJA 2011 drying
499 and warming that essentially matches that observed with the modeled warming clearly aided
500 by greenhouse-induced warming. In a similar analysis for Texas alone (which is a subset of
501 our larger domain) Hoerling et al. (2013) found that 2011 was a true outlier with temper-
502 atures well above the temperature-precipitation line and concluded that background global
503 warming likely was responsible for the warming above what would be expected given the
504 precipitation reduction. This is not so striking for the larger region considered here but

505 nonetheless appears to also be the case.

506 Another way of looking at the observed precipitation and temperature history is seen in
507 Figure 16 which shows the time history of JJA average observed temperature and precipita-
508 tion for 1950 to 2011 averaged over the TexMex region. Since temperature tends to rise when
509 precipitation goes down we have inverted the temperature scale here. The inverse relation
510 between the two quantities is also abundantly clear here with 2011 standing out as as having
511 the driest JJA and, hence, the warmest one too. The hot and dry summer of 1980 is also
512 clear here but as an isolated one year event. The string of hot dry summers in the 1950s is
513 also clear as well as the cooler and wetter extended period from the mid 1960s through the
514 mid 1990s. Amidst considerable seasonal to decadal variability, neither temperature nor pre-
515 cipitation in the TexMex region have a clear trend. However the TexMex region is expected
516 to get drier as a consequence of greenhouse gas-driven global warming, according to climate
517 models (Seager et al. 2007; Seager and Vecchi 2010) but it is quite likely that that trend
518 is currently masked by the presence of large amplitude natural variability on interannual to
519 multidecadal timescales (Hoerling et al. 2013).

520 **9. How well was the 2010/11 drought forecast by oper-** 521 **ational seasonal-to-interannual prediction systems?**

522 Understanding the dynamical causes of droughts is important but more important from
523 the point of view of planning ahead for, and possibly preventing, damaging impacts is de-
524 velopment of an ability to predict droughts. Of course this will not always be possible.
525 Indeed the analysis so far of the causes of the 2010/11 TexMex drought would suggest that
526 it would not have been well predicted ahead of time. After all, prediction of drought on the
527 seasonal-to-interannual timescale will depend on the ability to predict slowly evolving bound-
528 ary conditions that, by forcing the atmospheric circulation, can create tendencies towards
529 drought-inducing patterns of sufficient amplitude that they can emerge amidst the internal
530 atmospheric variability. SSTs and soil moisture anomalies are the boundary conditions to
531 be predicted, with the former the one that has been best shown to provide predictability.

532 However, our analysis has shown that the 2010/11 drought was at best only loosely linked
533 to SST anomalies so we would not expect a very skillful prediction.

534 The International Research Institute for Climate and Society (IRI) produces each month
535 seasonal forecasts of precipitation based on predictions of the evolving ocean state and
536 the atmospheric response to it. The realtime forecasts issued by the IRI (i.e. the 'Net
537 Assessments') over the United States are taken from the operational forecasts from the
538 Climate Prediction Center (CPC) of the National Weather Service in which the multi-model
539 ensemble product from the IRI (Barnston et al. 2010)² is one input. Here we just present
540 the IRI multi-model ensemble results for the global SST and North American precipitation
541 forecasts but adopt the same plotting conventions as for the publicly issued Net Assessment
542 forecasts, i.e. probabilities of precipitation amounts falling within terciles of the distributions,
543 as opposed to actual amounts, and limit ourselves to a qualitative comparison with what
544 actually occurred. In Figures 17 and 18 we show the 3.5 month lead time forecasts of seasonal
545 means from SON 2010 through SON 2011. Looking at the SST forecasts first, which can be
546 compared to the observed SST anomalies in Figure 4, it is clear the the La Niña conditions
547 in the Pacific Ocean during winter 2010/11 were quite well forecast with a 3.5 month lead.
548 The warmth of the Atlantic Ocean was, however, not well forecast. The forecast then had
549 the La Niña persist at strength into MAM 2011 whereas in nature the event was already
550 significantly decayed by then. The forecast did not have the La Niña decay until SON 2011
551 but by then, in nature, the weakened La Niña had already begun to strengthen again.

552 Turning now to the precipitation forecasts, which can be compared against observed
553 precipitation anomalies shown in Figure 5, there was considerable skill from SON 2010
554 through MAM 2011. The 3.5 month forecast for DJF 2010/11 confidently predicted a 40
555 to 50 % chance of drier than normal conditions (lowest tercile) across the southern U.S.
556 and northern Mexico clearly matching the observed anomaly. The forecast also successfully
557 predicted continued dry conditions in MAM 2011. These precipitation forecasts were driven
558 by the largely successful prediction of La Niña conditions from SON 2010 through MAM

²The IRI two-tier forecast system uses a product based on the combination of 3 different SST predictions (from both dynamical and statistical methods and persistence) to force a variety of atmosphere GCMs to create a multi-scenario, multimodel ensemble which is used to generate the precipitation forecasts.

559 2011. However, as noted in Section 6, the observed precipitation reductions in the southeast
560 U.S. seem to have been associated with the negative NAO event and, hence, it seems the
561 forecast skill in that region is partly luck. For JJA 2011, despite the forecast of continued La
562 Niña conditions, the precipitation forecast for North America was for climatological amounts.
563 This is consistent with teleconnections between tropical Pacific SST anomalies and North
564 American precipitation in the summer season being insufficiently robust to provide predictive
565 skill. As such, the forecasts failed to predict the serious near pan-continental drought of
566 summer 2011. As the La Niña redeveloped in SON 2011, and the forecast also predicted
567 weak La Niña conditions, the seasonal reestablishment of teleconnections transferred this
568 into forecasts of modest likelihood of drier than normal conditions which was in line with
569 what occurred.

570 Despite the inability to predict the severe dry anomalies of summer 2011, consistent with
571 the limited influence of SSTs on North American hydroclimate in the summer, the 3.5 month
572 forecasts nonetheless warned of an impending and developing drought. If we recall that in
573 summer 2010 the U.S. was essentially free of drought according to the Drought Monitor, the
574 forecast from spring and summer 2010 that the southern U.S. and Mexico would immediately
575 move back into drier than normal conditions was prescient and provided useful information,
576 with seasonal forewarning, for any efforts in drought planning.

577 **10. Conclusions**

578 We have attempted to determine the causes of the 2010-11 severe drought in North
579 America which was centered on the regions of Texas and northeastern Mexico and which
580 had severe social consequences. Our conclusions are as follows:

- 581 • The drought began in fall of 2010 just as a La Niña developed in the tropical Pacific
582 Ocean and was concurrent with La Niña conditions through to fall of 2011 when our
583 analysis ends. Historically, severe and extended droughts in the southwest U.S, Plains
584 and northern Mexico have coincided with La Niña conditions and, in that sense, the
585 recent drought appears the latest such event.

- 586 • Climate models forced by observed SSTs, produce drought conditions across the south-
587 ern U.S. and northern Mexico from fall 2010 to spring 2011 which coincides with
588 the seasons when tropical Pacific SSTs are most effective in exciting a teleconnected
589 atmospheric circulation response over North America. In summer 2011 the models
590 produce much weaker precipitation reductions than those observed which, while con-
591 sistent with low teleconnectivity to the tropical Pacific in summer, and an important
592 role for internal atmospheric variability in the observations, could also indicate weak
593 local land-atmosphere interactions in the models.
- 594 • Despite the model support for tropical Pacific SSTs as the cause of the onset and
595 continuation of the drought, detailed analysis of precipitation and mean and tran-
596 sient atmospheric circulation fields provides evidence that the actual drought was also
597 strongly influenced by internal atmospheric variability that caused departures of these
598 patterns from those typically associated with La Niña conditions. For example during
599 winter 2010/11 a very strong negative NAO event caused northerly and descending
600 flow over the southern Plains and southeast U.S. inducing drying.
- 601 • The decomposed moisture budgets in the models and Reanalyses provide better indica-
602 tion of the mechanisms involved in the drought. In the models during winter 2010/11
603 the drought intensifies over much of the southern U.S. due to anomalous moisture di-
604 vergence by transient eddies which is related to the canonical northward shift of the
605 Pacific-North America storm track expected during La Niña events. In the Reanalyses
606 drying by transient eddies is much more spatially diffuse. However, the ERA-Interim
607 does show strong drying over Texas, the south central and southeastern U.S. due to
608 mean flow moisture divergence associated with the negative NAO event. The Reanal-
609 yses agree that mean flow moisture divergence anomalies sustain the drought in the
610 summer of 2011 but this is not captured by the SST-forced models.
- 611 • The inability of the models to reproduce the observed precipitation and circulation
612 anomalies as a consequence of SST-forcing alone could be in part a result of model
613 error but also suggests that random internal atmospheric variability played a significant
614 role in the character, timing and evolution of this particular drought. This limits

615 predictability of the drought, even in the winter season when North America is most
616 influenced by tropical Pacific SST anomalies and even when, as in winter 2010/11 the
617 SST anomalies were strong. Continuation of the drought into summer 2011 appears
618 unpredictable in terms of the weakening La Niña SST anomalies and could have arisen
619 also from random internal atmospheric variability. However, the role of soil moisture-
620 atmosphere interactions should also be examined and whether these are adequately
621 captured in climate models.

622 • Realtime predictions performed by the IRI did successfully predict drought over the
623 southern U.S. and northern Mexico to develop in SON 2010 and to intensify and persist
624 through MAM 2011 which was based on successful forecasts of La Niña conditions.
625 However, given the role of the NAO in the observed winter 2010/11 drought, the
626 mechanisms of the forecast drought probably differed in details from the actual drought.
627 The SST forecasts continued the La Niña into summer 2011 but this did not translate
628 into a drought forecast and the actual drought in summer was not predicted.

629 • The high (and record-breaking) surface air temperatures during summer 2011 in the
630 TexMex region are consistent with the very dry conditions and the general and clear
631 inverse relation between precipitation and temperature in the region over past decades.
632 Summer 2011 appears as extreme in terms of its dryness and warmth but not necessarily
633 outside the range expected from this relation alone.

634 The 2010/11 drought has extended into fall of 2012 with another summer of record
635 breaking heat and drought as well as the extension of the drought into both the southwest and
636 the midwest. La Niña conditions also persisted from 2011 to 2012 before fading in summer
637 of 2012. Follow up work will be needed to assess the cause of the 2011/12 drought but, as for
638 the prior year, a combination of SST-forced and internally generated atmospheric circulation
639 and moisture budget anomalies are likely the cause. The possibility that temperature records
640 have been broken because background global warming is adding on to the high temperatures
641 caused by dry conditions also needs to be addressed (Hoerling et al. 2013). In terms of
642 seasonal-to-interannual prediction, successful prediction of tropical Pacific SSTs can enable
643 a prediction of emerging or continuing dry conditions during the northern hemisphere fall,

644 winter and spring seasons. However extremes are rarely, if ever, predicted as a most-likely
645 outcome. Nonetheless, the summer drought conditions appeared essentially unpredictable
646 with current prediction systems. It should be remembered that in some cases atmospheric
647 variability will offset the impacts of SST-forced anomalies; in other cases they will enhance
648 the SST-forced anomalies. However, in the case of 2010/11, the combination of La Niña
649 conditions and internal atmospheric variability led to a drought that was severe, much worse
650 in terms of dryness and heat than that forecast ahead of time and at the very edge of the
651 observed natural variability of climate.

652 *Acknowledgments.*

653 This work was supported by NOAA awards NA08OAR4320912 and NA10OAR4310137
654 (Global Decadal Hydroclimate Variability and Change) and NSF award AGS-0804107. The
655 authors thank Yochanan Kushnir for useful discussions and Shuhua Li for help with the IRI
656 forecast data.

REFERENCES

- 659 Barnston, A., S. Li, S. J. Mason, D. G. DeWitt, L. Goddard, and X. Gong, 2010: Verification
660 of the First 11 Years of IRIs Seasonal Climate Forecasts. *J. Appl. Meteor. Clim.*, **49**, 493–
661 520.
- 662 Chen, J., B. E. Carlson, and A. D. Del Genio, 2002: Evidence for strengthening of the
663 tropical general circulation in the 1990s. *Science*, **295**, 838–841.
- 664 Cook, B., R. Miller, and R. Seager, 2008: Dust and sea surface temperature forcing of the
665 Dust Bowl drought. *Geophys. Res. Lett.*, **35**, doi:10.1029/2008GL033486.
- 666 Cook, B., R. Miller, and R. Seager, 2009: Amplification of the North American Dust Bowl
667 drought through human-induced land degradation. *Proc. Nat. Acad. Sci.*, **106**, 4997–5001.
- 668 Cook, B., R. Seager, and R. Miller, 2010: Atmospheric circulation anomalies during two
669 persistent North American droughts: 1932-39 and 1948-57. *Clim. Dyn.*, 4997–5001.
- 670 Dee, D., et al., 2011: The ERA-Interim Reanalysis; configuration and performance of the
671 data assimilation system. *Quart. J. Roy. Meteor. Soc.*, **137**, 553–597.
- 672 Herweijer, C., R. Seager, and E. R. Cook, 2006: North American droughts of the mid to
673 late Nineteenth Century: History, simulation and implications for Medieval drought. *The
674 Holocene*, **16**, 159–171.
- 675 Hoerling, M. P., X.-W. Quan, and J. Eischeid, 2009: Distinct causes for two principal U.S.
676 droughts of the 20th century. *Geophys. Res. Lett.*, **36**, doi:10.1029/2009GL039860.
- 677 Hoerling, M. P., et al., 2013: Anatomy of an extreme event. *J. Climate.*, in press.
- 678 Jin, E. K., et al., 2008: Current status of ENSO prediction skill in coupled ocean-atmosphere
679 models. *Clim. Dyn.*, **31**, 647–664.

680 Kalnay, E. et al., 1996: The NCEP/NCAR 40-year reanalysis project. *Bull. Am. Meteor.*
681 *Soc.*, **77**, 437–471.

682 Kaplan, A., M. A. Cane, Y. Kushnir, A. C. Clement, M. B. Blumenthal, and B. Rajagopalan,
683 1998: Analyses of global sea surface temperature: 1856-1991. *J. Geophys. Res.*, **103**,
684 18 567–18 589.

685 Kistler, R., et al., 2001: The NCEP-NCAR 50-year Reanalysis: Monthly means CD-ROM
686 and documentation. *Bull. Am. Meteor. Soc.*, **82**, 247–268.

687 Mason, S. and L. Goddard, 2001: Probabilistic precipitation anomalies associated with enso.
688 *Bull. Amer. Meteor. Soc.*, 619–638.

689 Rayner, N., D. Parker, E. Horton, C. Folland, L. Alexander, D. Rowell, E. Kent, and A. Ka-
690 plan, 2003: Global analyses of sea surface temperature, sea ice, and night marine air tem-
691 perature since the late nineteenth century. *J. Geophys. Res.*, **108**, 10.1029/2002JD002 670.

692 Roeckner, E. K., et al., 1996: The atmospheric general circulation model ECHAM-4: Model
693 description and simulation of present day climate. Tech. Rep. 218, Max-Planck-Institut
694 für Meteorologie, 90 pp.

695 Ropelewski, C. F. and M. S. Halpert, 1986: North American precipitation and temperature
696 patterns associated with the El Niño/Southern Oscillation. *Mon. Wea. Rev.*, **114**, 2352–
697 2362.

698 Schubert, S. D., M. J. Suarez, P. J. Pegion, R. D. Koster, and J. T. Bacmeister, 2004a:
699 Causes of long-term drought in the United States Great Plains. *J. Climate*, **17**, 485–503.

700 Schubert, S. D., M. J. Suarez, P. J. Pegion, R. D. Koster, and J. T. Bacmeister, 2004b: On
701 the cause of the 1930s Dust Bowl. *Science*, **303**, 1855–1859.

702 Schubert, S. D., et al., 2009: A U.S. Clivar project to assess and compare the responses of
703 global climate models to drought-related SST forcing patterns: Overview and results. *J.*
704 *Climate*, **22**, 5251– 5272.

705 Seager, R., 2007: The turn-of-the-century North American drought: dynamics, global con-
706 text and prior analogues. *J. Climate*, **20**, 5527–5552.

707 Seager, R., N. Harnik, Y. Kushnir, W. Robinson, and J. Miller, 2003: Mechanisms of hemi-
708 spherically symmetric climate variability. *J. Climate*, **16**, 2960–2978.

709 Seager, R., N. Harnik, W. A. Robinson, Y. Kushnir, M. Ting, H. P. Huang, and J. Velez,
710 2005a: Mechanisms of ENSO-forcing of hemispherically symmetric precipitation variabil-
711 ity. *Quart. J. Roy. Meteor. Soc.*, **131**, 1501–1527.

712 Seager, R. and N. Henderson, 2013: Diagnostic computation of moisture budgets in atmo-
713 sphere models with reference to analysis of CMIP archived data. *J. Climate*, submitted.

714 Seager, R., Y. Kushnir, C. Herweijer, N. Naik, and J. Velez, 2005b: Modeling of tropical
715 forcing of persistent droughts and pluvials over western North America: 1856-2000. *J.*
716 *Climate*, **18**, 4068–4091.

717 Seager, R., Y. Kushnir, M. Ting, M. A. Cane, N. Naik, and J. Velez, 2008: Would advance
718 knowledge of 1930s SSTs have allowed prediction of the Dust Bowl drought? *J. Climate*,
719 **21**, 3261–3281.

720 Seager, R., N. Naik, M. A. Cane, N. Harnik, M. Ting, and Y. Kushnir, 2010: Adjustment
721 of the atmospheric circulation to tropical Pacific SST anomalies: Variability of transient
722 eddy propagation in the Pacific-North America sector. *Quart. J. Roy. Meteorol. Soc.*,
723 **136**, 277–296.

724 Seager, R. and G. A. Vecchi, 2010: Greenhouse warming and the 21st Century hydroclimate
725 of southwestern North America. *Proc. Nat. Acad. Sci.*, **107**, 21 277–21 282.

726 Seager, R., et al., 2007: Model projections of an imminent transition to a more arid climate
727 in southwestern North America. *Science*, **316**, 1181–1184.

728 Seager, R., et al., 2009: Mexican drought: An observational, modeling and tree ring study
729 of variability and climate change. *Atmosfera*, **22**, 1–31.

- 730 Stahle, D. W. and M. K. Cleaveland, 1988: Texas drought history reconstructed and analyzed
731 from 1698 to 1980. *J. Climate*, **1**, 59–74.
- 732 Stahle, D. W., et al., 2009: Early 21st century drought in Mexico. *EOS*, **90**, 89–100.
- 733 Strauss, D. M. and J. Shukla, 2002: Does ENSO force the PNA? *J. Climate*, **15**, 2340–2358.

734 Table 1. Anomaly correlation coefficients between observed and modeled precipitation
 735 anomalies for the $20^{\circ}N$ to $50^{\circ}N$ region, land areas only, accounting for area weighting.

	SON 2010	DJF 2010/11	MAM 2011	JJA 2011	SON 2011
Obs-CCM3	0.05	0.45	0.33	0.03	-0.30
Obs-ECHAM	0.43	0.41	0.63	0.32	-0.03
CCM3-ECHAM	0.34	0.56	0.69	0.60	0.15

736 List of Figures

737	1	The observed SST, precipitation (over land only) and 200mb heights com-	
738		posited over La Niña events by season. Units are Kelvin, mm/month and	
739		geopotential meters.	32
740	2	As for Figure 1 but for the CCM3 model simulations	33
741	3	As for Figure 1 but for the ECHAM4.5 model simulations.	34
742	4	The history of SST (over ocean) and surface air temperature (over land) during	
743		the 2010/11 TexMex drought shown in 3 month averages from September to	
744		November 2010 to September to November 2011. Units are Kelvin.	35
745	5	The observed (left) and modeled with the CCM3 (middle) and ECHAM4.5	
746		(right) model precipitation anomalies by season during the 2010/11 TexMex	
747		drought. Units are mm/day.	36
748	6	The modeled moisture budget anomalies for the CCM3 models (top four pan-	
749		els) and the ECHAM4.5 model (bottom forum panels). In each coup of four	
750		panels the model precipitation anomaly is at top left, the evaporation anomaly	
751		at top right, the vertically integrated mean flow moisture convergence anomaly	
752		at bottom left and the vertically integrated transient eddy moisture conver-	
753		gence anomaly at bottom right. Results are for fall (SON) of 2010. All panels	
754		are in units of mm/day.	37
755	7	Same as Figure 3 but for DJF 2010/11.	38
756	8	Same as Figure 3 but for MAM 2011.	39
757	9	Same as Figure 3 but for JJA 2011.	40
758	10	Same as Figure 3 but for SON 2011.	41
759	11	Anomalies of the convergence of the vertically integrated moisture transport	
760		in the NCEP-NCAR Reanalysis due to (left) anomalies in the monthly mean	
761		state and (right) the covariance of the sub-monthly transient states for the	
762		seasons of the 2010/11 drought.	42

763	12	Same as Figure 8 but using the ERA-Interim Reanalysis (relative to a 1979	
764		to 2011 climatology. The monthly mean state and transient contributions are	
765		in the middle and right columns, respectively while the left column shows the	
766		anomalies in the convergence of the vertically integrated moisture transports	
767		as reported within the ERA-Interim data and which is well approximated by	
768		the sum of the two contributions.	43
769	13	The 200mb geopotential height anomalies for the seasons from SON 2010 to	
770		SON 2011 for the NCEP-NCAR Reanalysis (left), the CCM3 model (middle)	
771		and the ECHAM4.5 model (right). Heights were detrended to remove an	
772		overall increase caused by global warming. Units are meters.	44
773	14	Same as Figure 8 (with no detrending) but for the 300mb sub monthly eddy	
774		meridional velocity variance. Units are meters squared per second squared.	45
775	15	Scatter plots of JJA temperature (Kelvin) and precipitation (mm/day) anoma-	
776		lies for the TexMex region and the 1950 to 2011 period for observations (top),	
777		the CCM3 model (middle) and the ECHAM4.5 model (bottom).	46
778	16	Time history of observed JJA temperature (bars, Kelvin) and precipitation	
779		(line, mm/day) anomalies for the TexMex region and the 1950 to 2011 period.	47
780	17	The 4 month lead time forecasts of SST (left) and North American precipita-	
781		tion (right) from the IRI seasonal-to-interannual prediction system for SON	
782		2010 from May 2010 (top), DJF 2010-11 from August 2010 (middle) and MAM	
783		2011 from November 2010 (bottom).	48
784	18	Same as Figure 13 but for forecasts of JJA 2011 from Febtuary 2011 (top)	
785		and SON 2011 from May 2011 (bottom).	49

Observed La Niña Composite 1950-2011

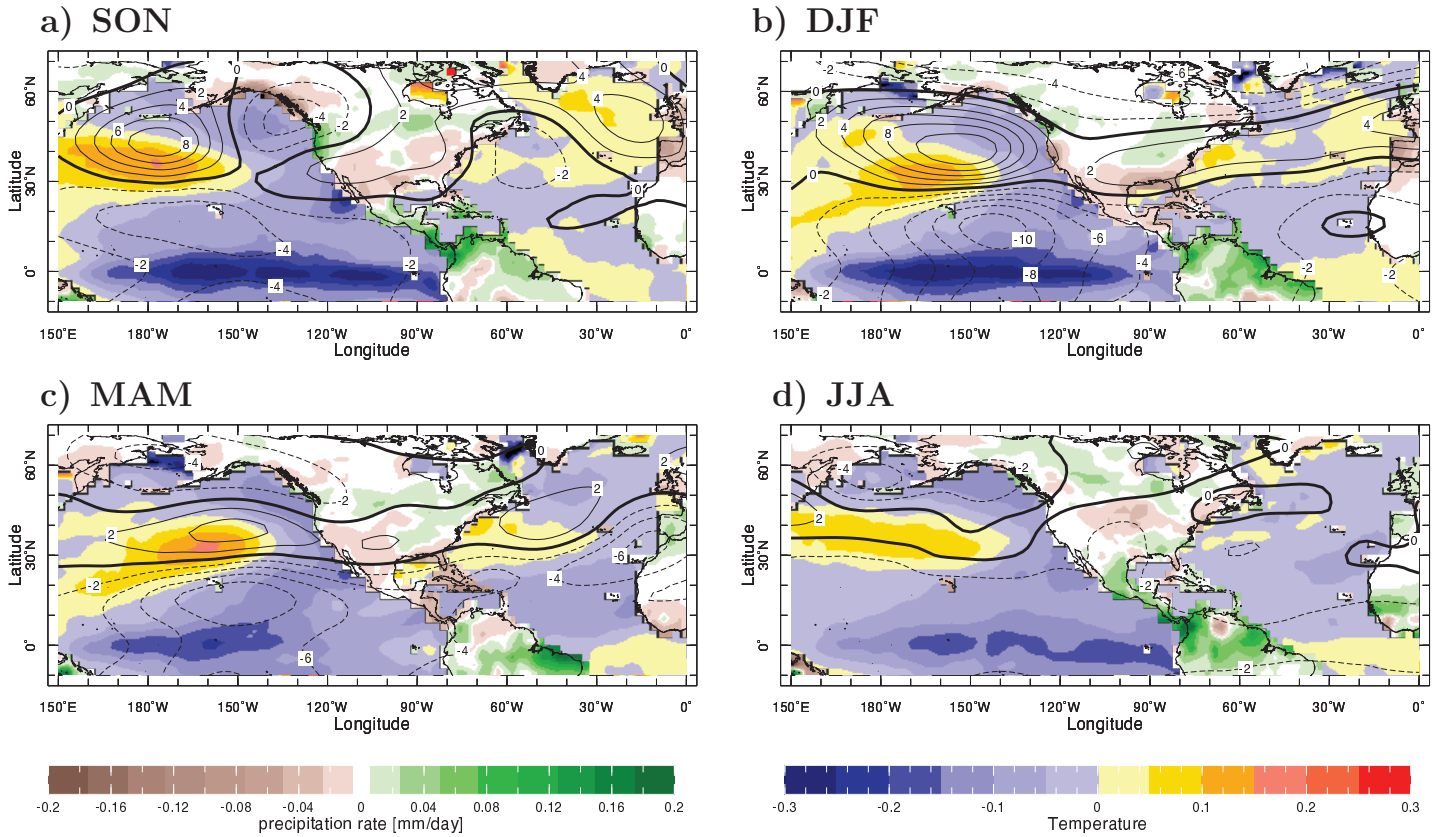


FIG. 1. The observed SST, precipitation (over land only) and 200mb heights composited over La Niña events by season. Units are Kelvin, mm/month and geopotential meters.

CCM3 La Niña Composite 1950-2011

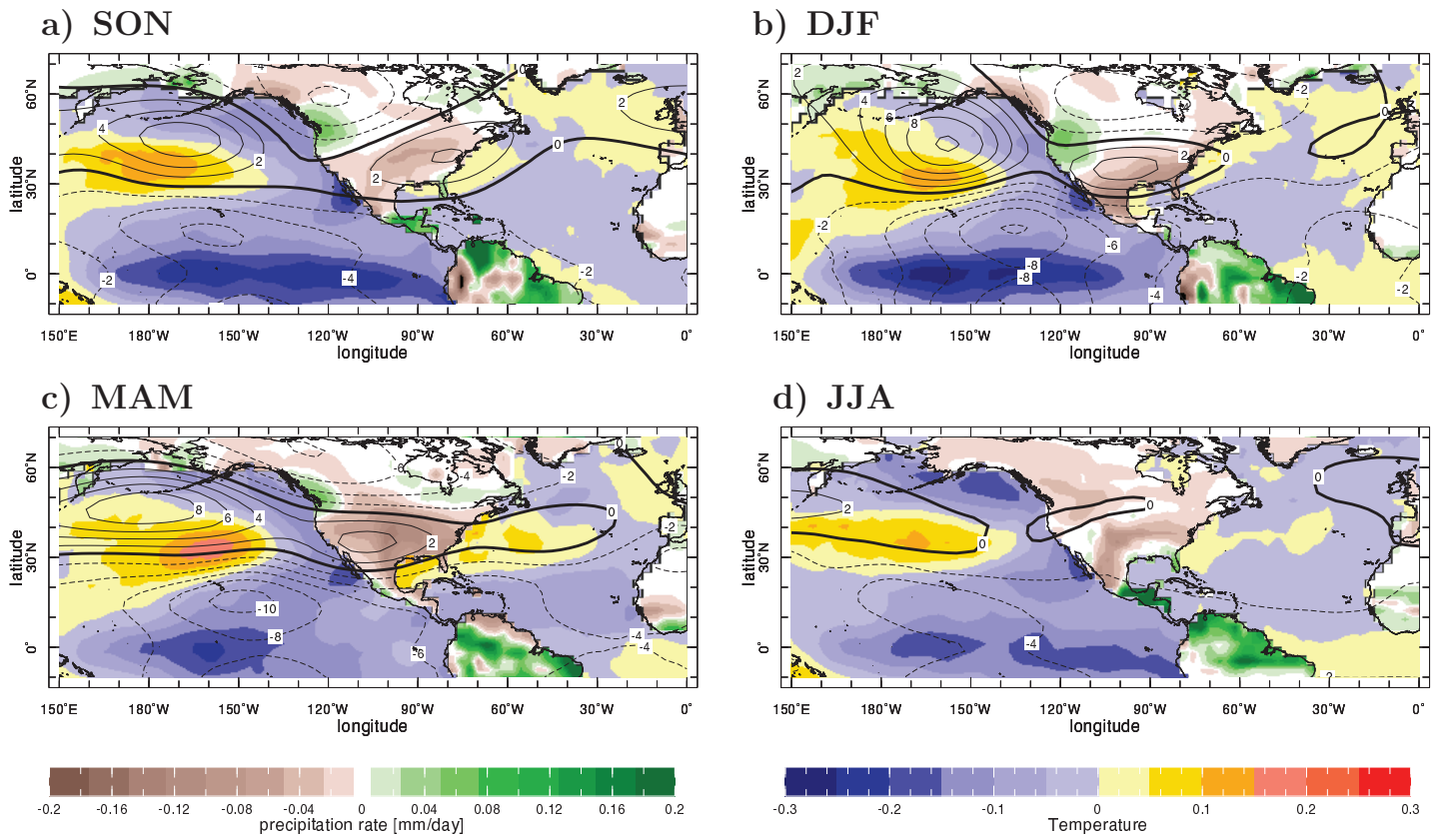


FIG. 2. As for Figure 1 but for the CCM3 model simulations

ECHAM 4.5 La Niña Composite 1950-2011

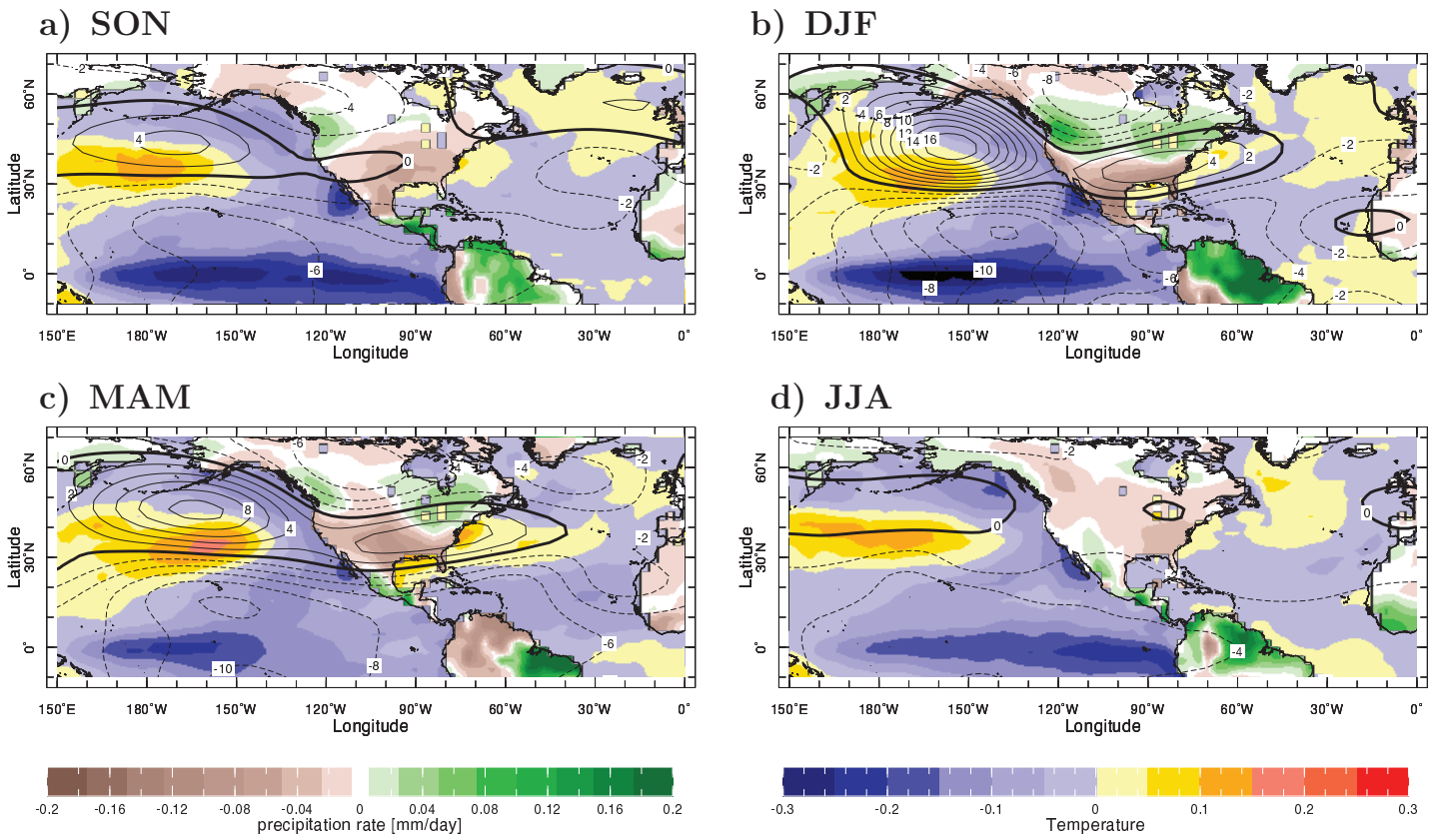


FIG. 3. As for Figure 1 but for the ECHAM4.5 model simulations.

SSTA (ocean), Surface Air Temp (land)

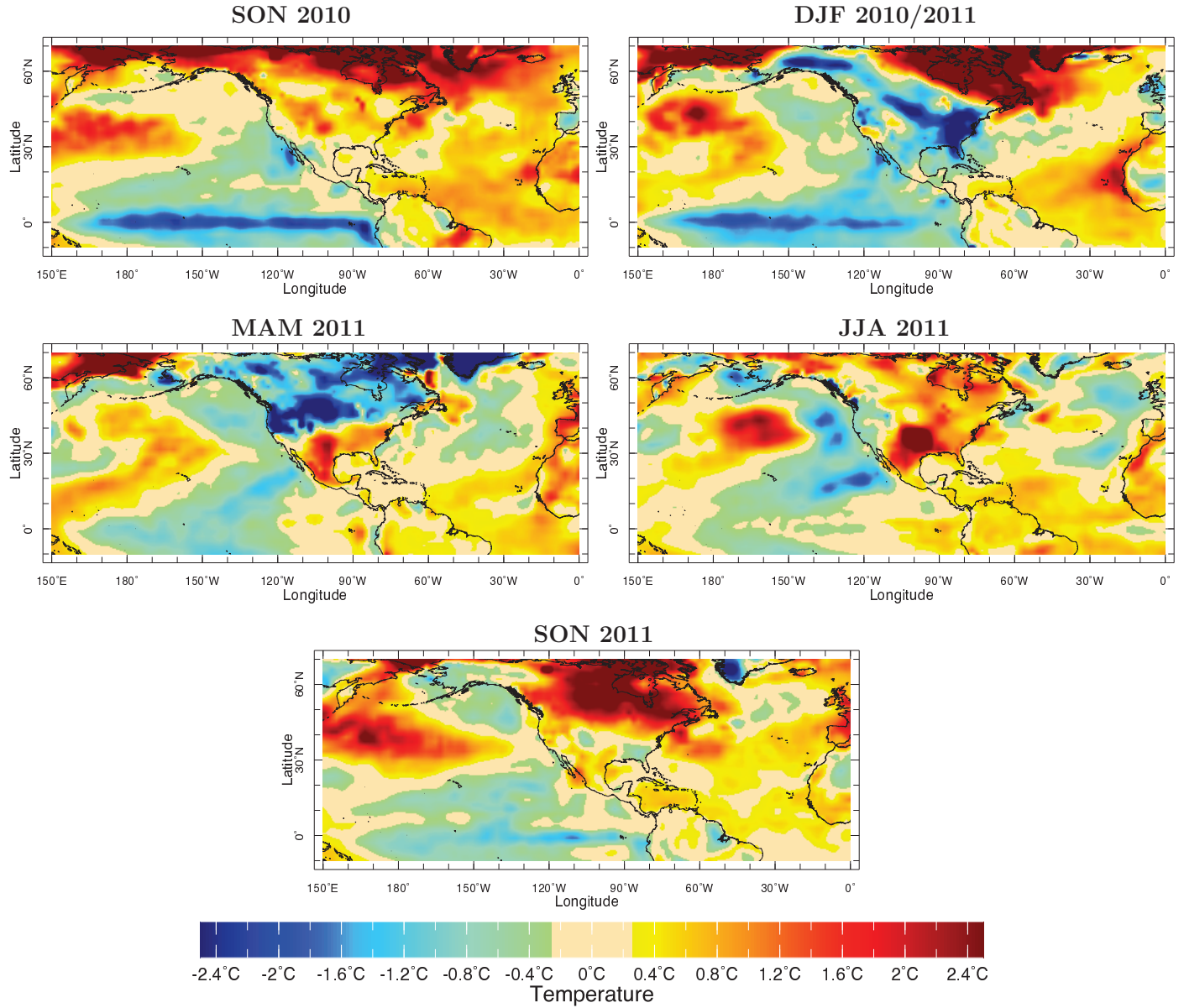


FIG. 4. The history of SST (over ocean) and surface air temperature (over land) during the 2010/11 TexMex drought shown in 3 month averages from September to November 2010 to September to November 2011. Units are Kelvin.

Precipitation Anomaly

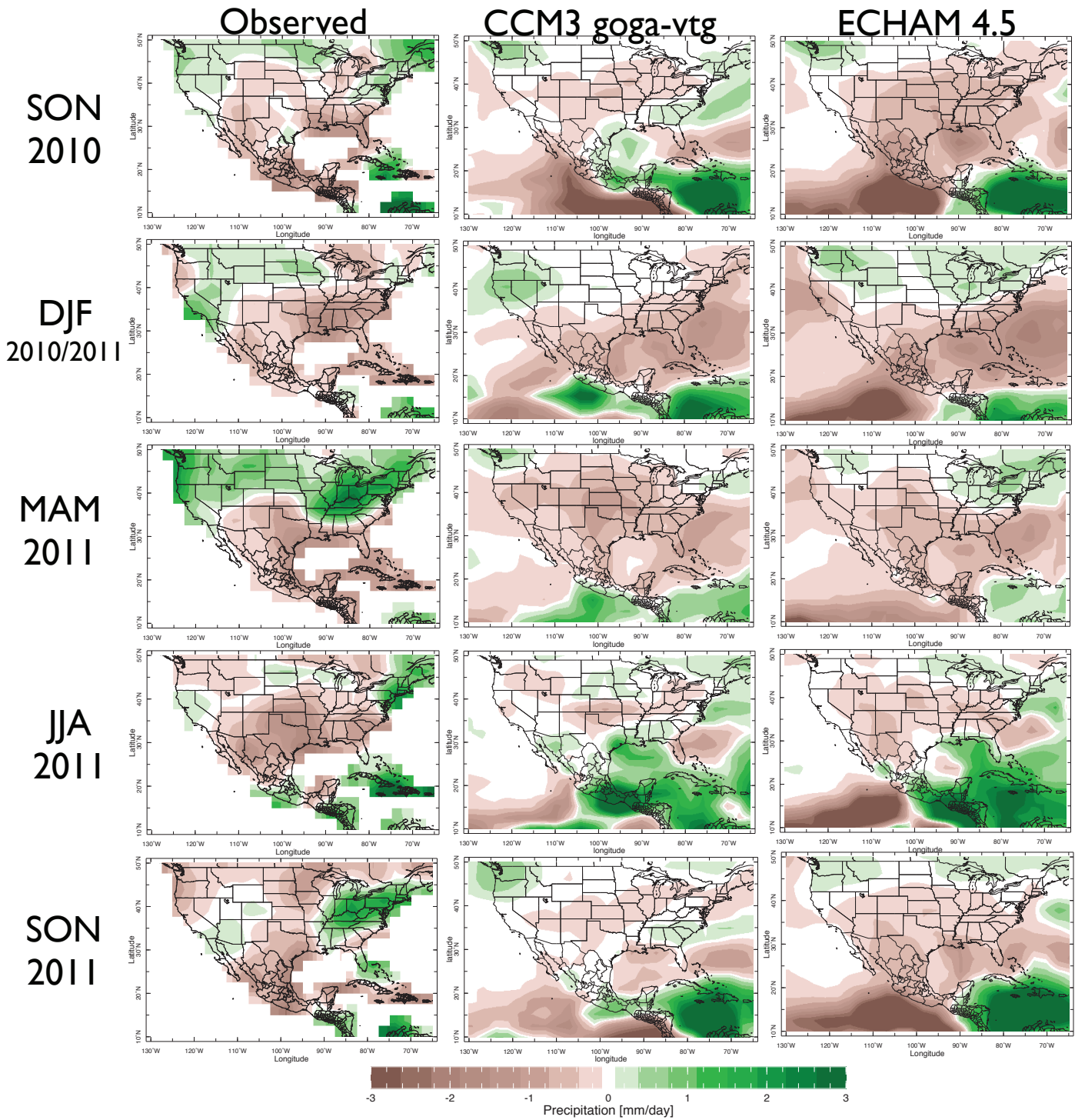
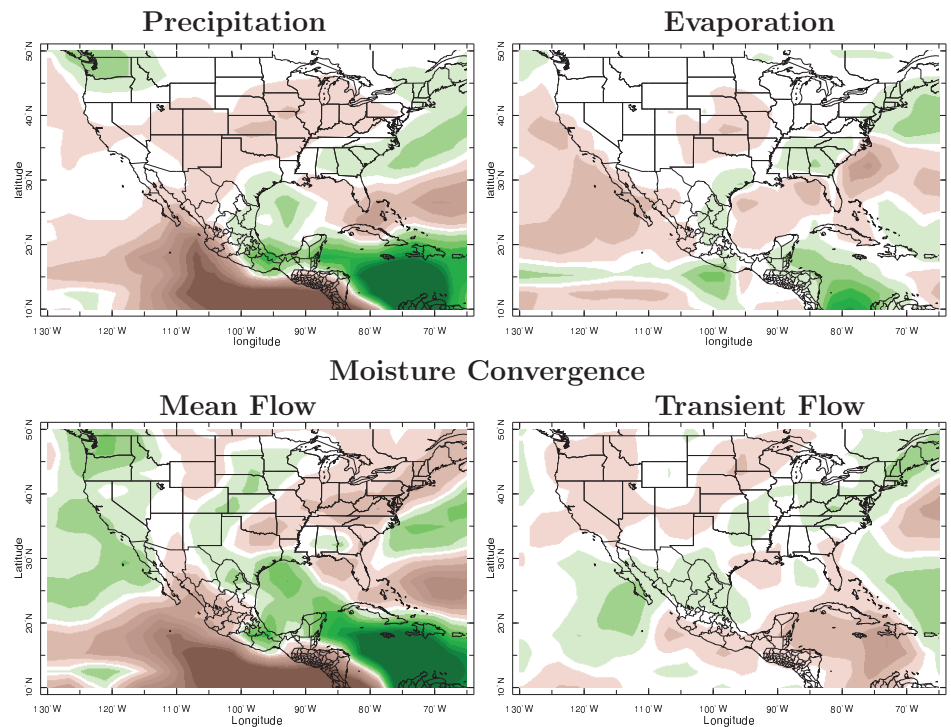


FIG. 5. The observed (left) and modeled with the CCM3 (middle) and ECHAM4.5 (right) model precipitation anomalies by season during the 2010/11 TexMex drought. Units are mm/day.

SON 2010 CCM3



ECHAM 4.5

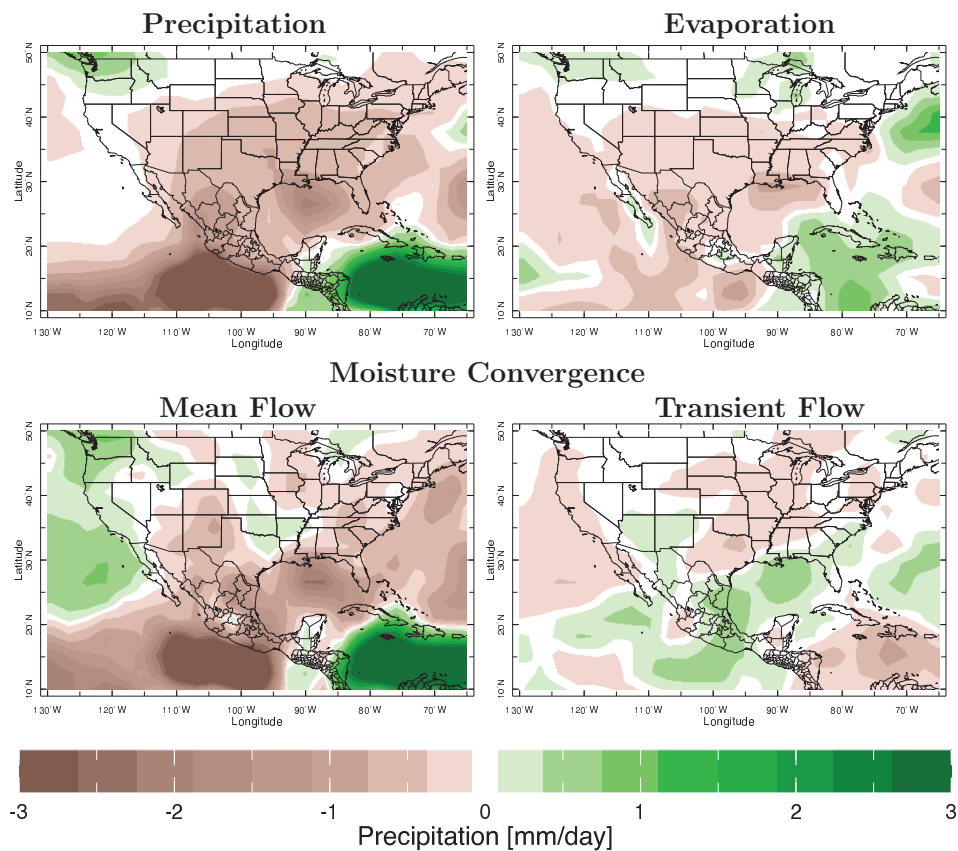
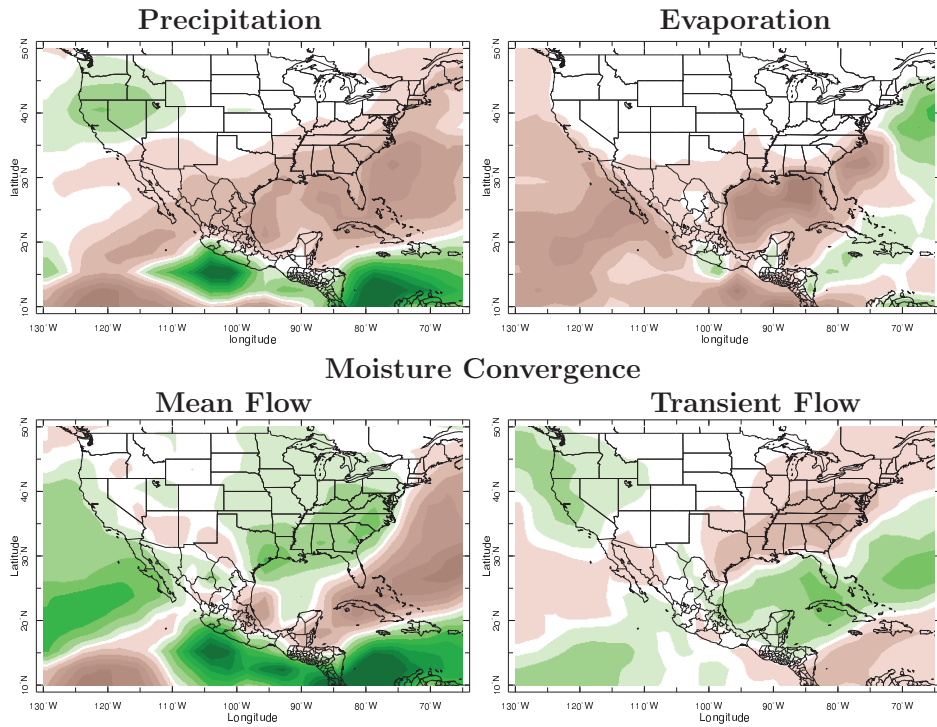


FIG. 6. The modeled moisture budget anomalies for the CCM3 models (top four panels) and the ECHAM4.5 model (bottom four panels). In each couple of four panels the model precipitation anomaly is at top left, the evaporation anomaly at top right, the vertically integrated mean flow moisture convergence anomaly at bottom left and the vertically integrated transient eddy moisture convergence anomaly at bottom right. Results are for fall (SON) of 2010. All panels are in units of mm/day.

DJF 2010/2011 CCM3



ECHAM 4.5

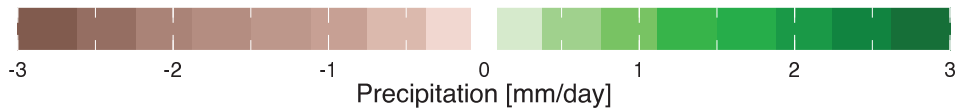
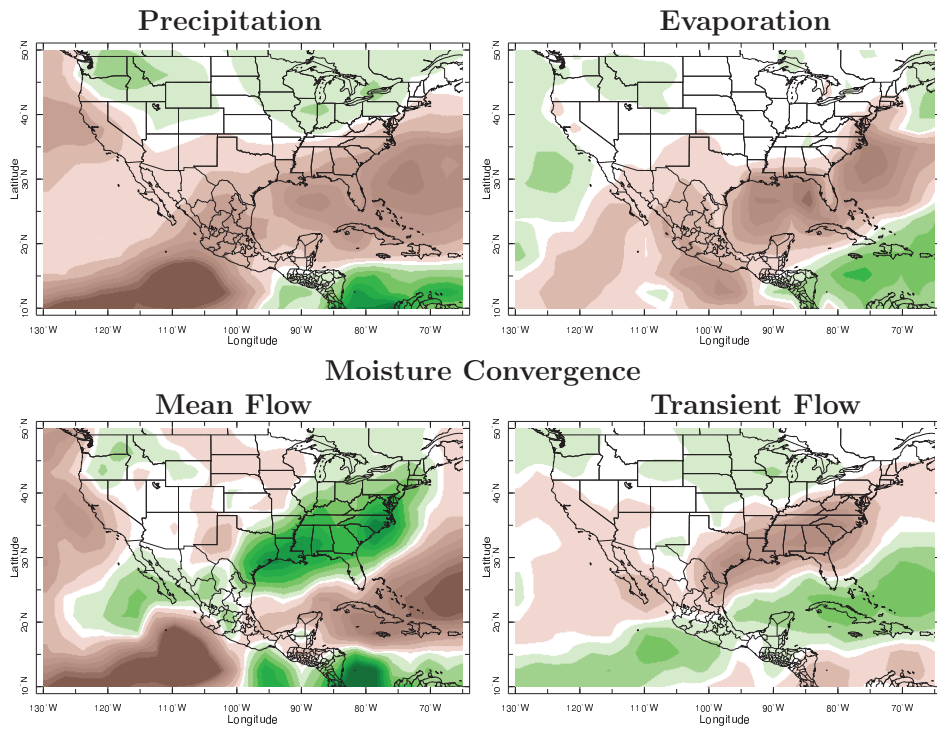
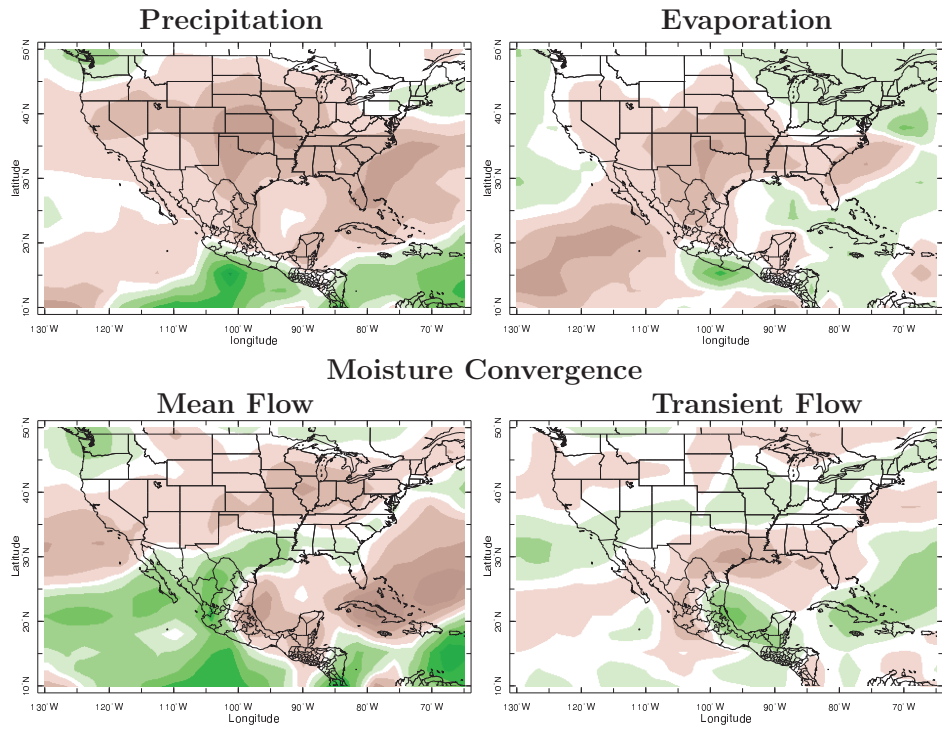


FIG. 7. Same as Figure 8 but for DJF 2010/11.

MAM 2011 CCM3



ECHAM 4.5

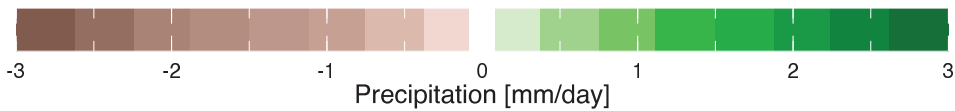
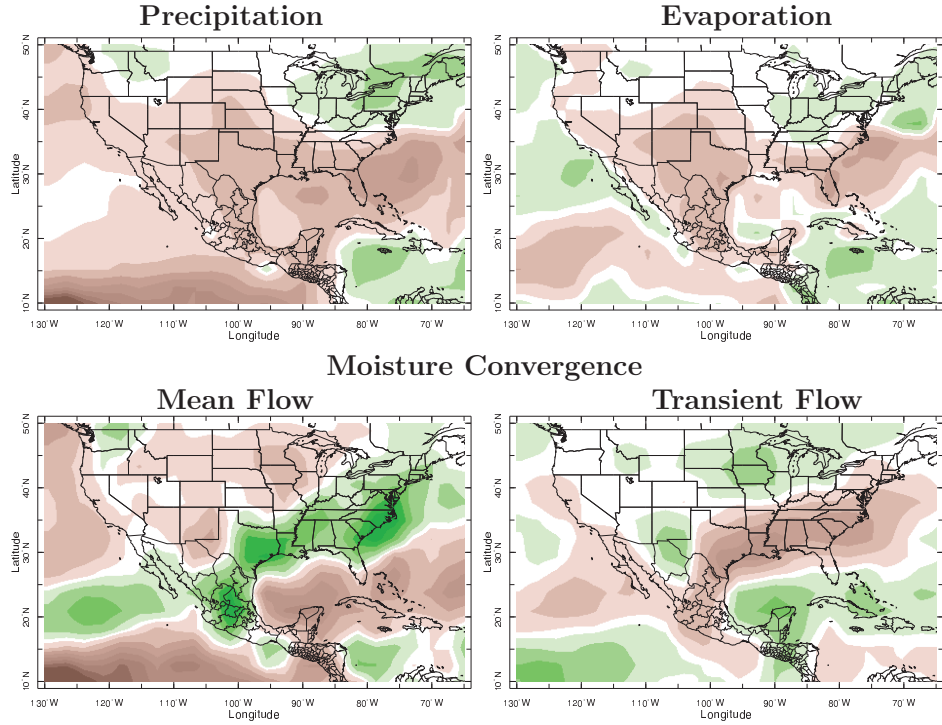
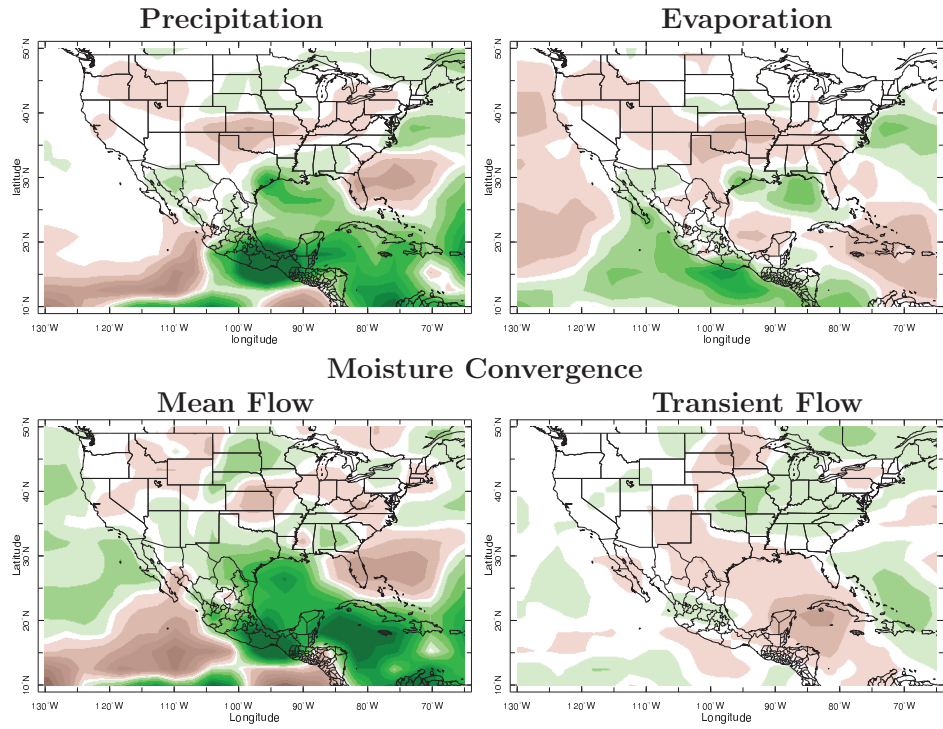


FIG. 8. Same as Figure 30.3 but for MAM 2011.

JJA 2011 CCM3



ECHAM 4.5

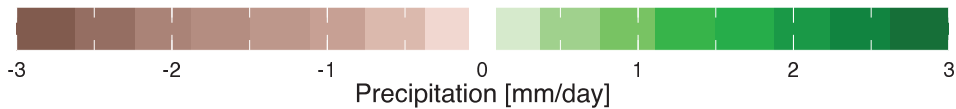
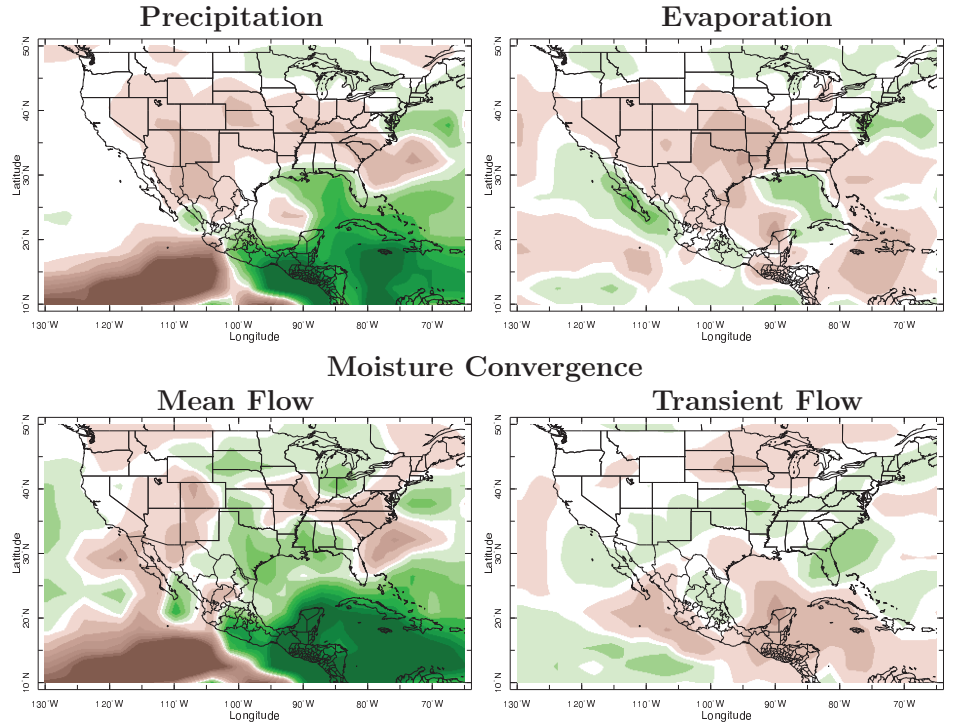
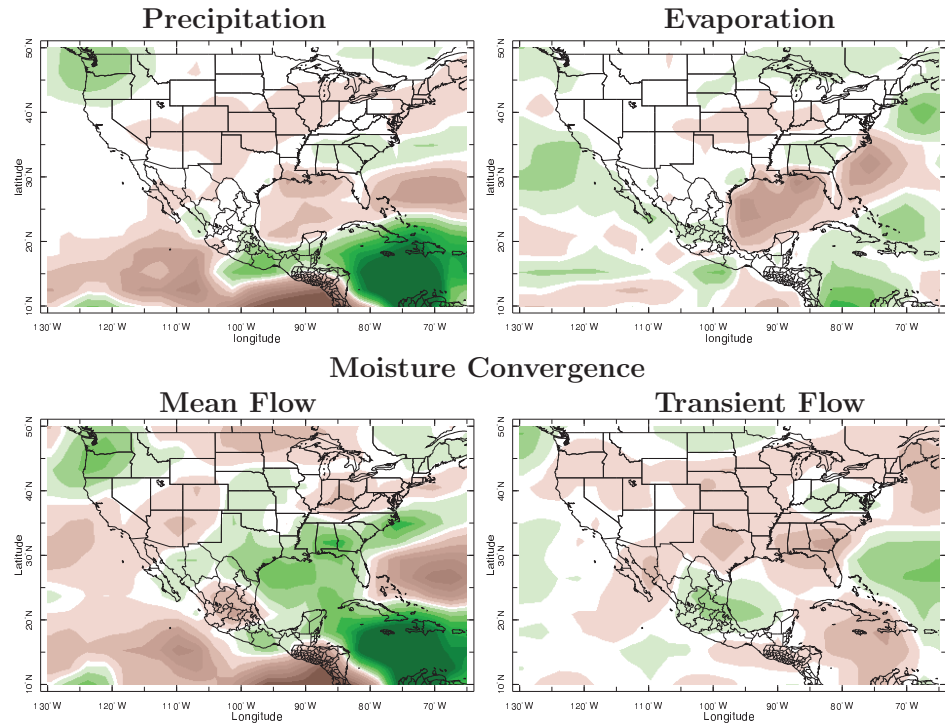


FIG. 9. Same as Figure 3 but for JJA 2011.

SON 2011 CCM3



ECHAM 4.5

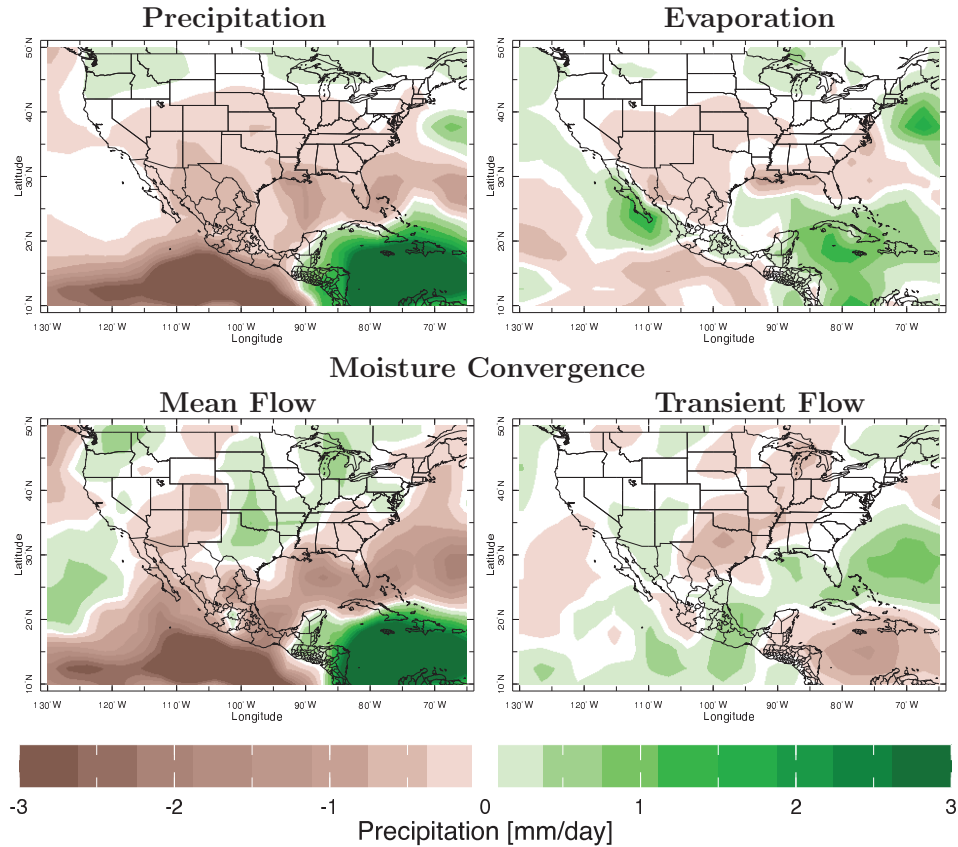


FIG. 10. Same as Figure 3 but for SON 2011.

NCEP

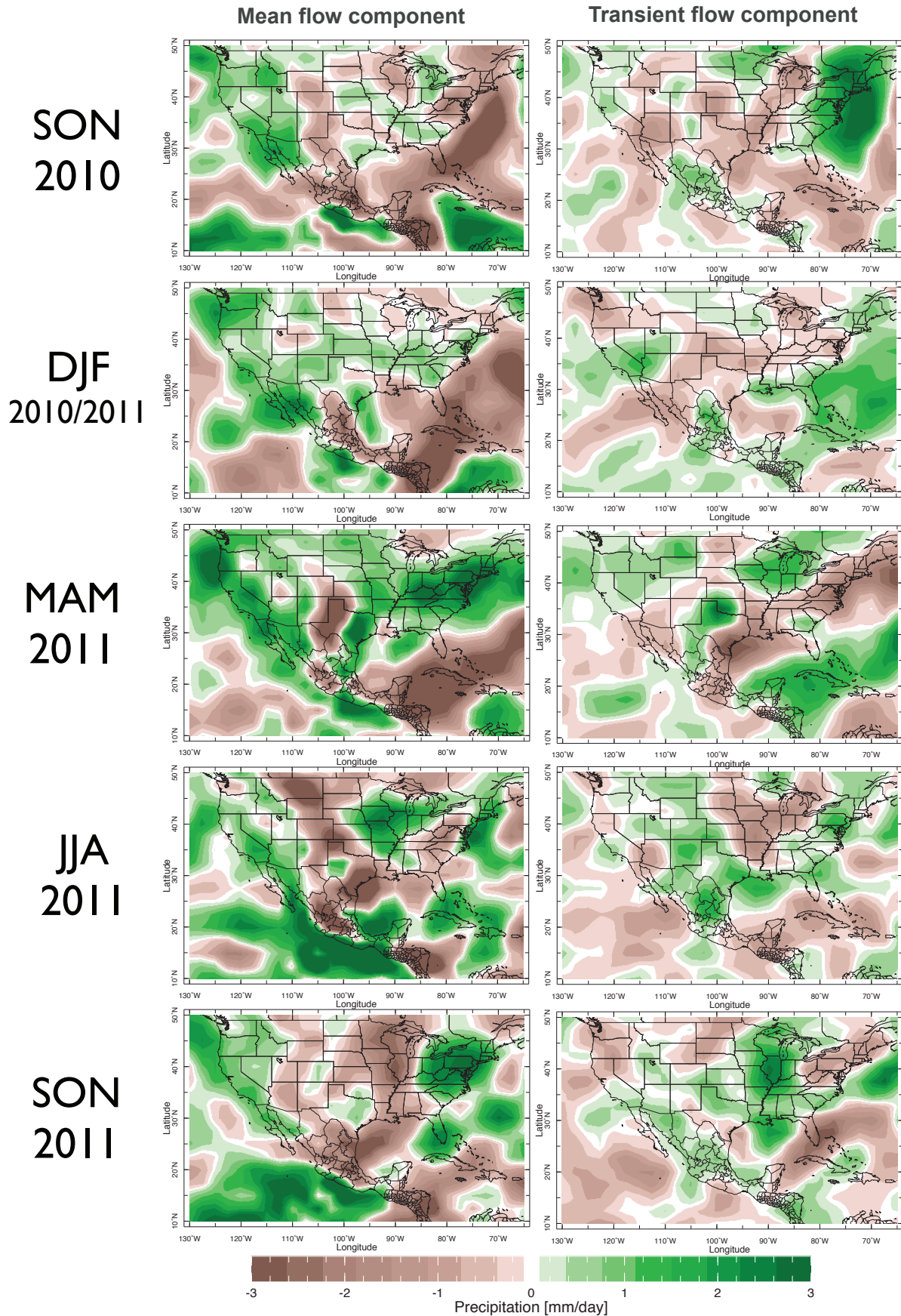


FIG. 11. Anomalies of the convergence of the vertically integrated moisture transport in the NCEP-NCAR Reanalysis due to (left) anomalies in the monthly mean state and (right) the covariance of the sub-monthly transient states for the seasons of the 2010/11 drought.

ERA-Interim

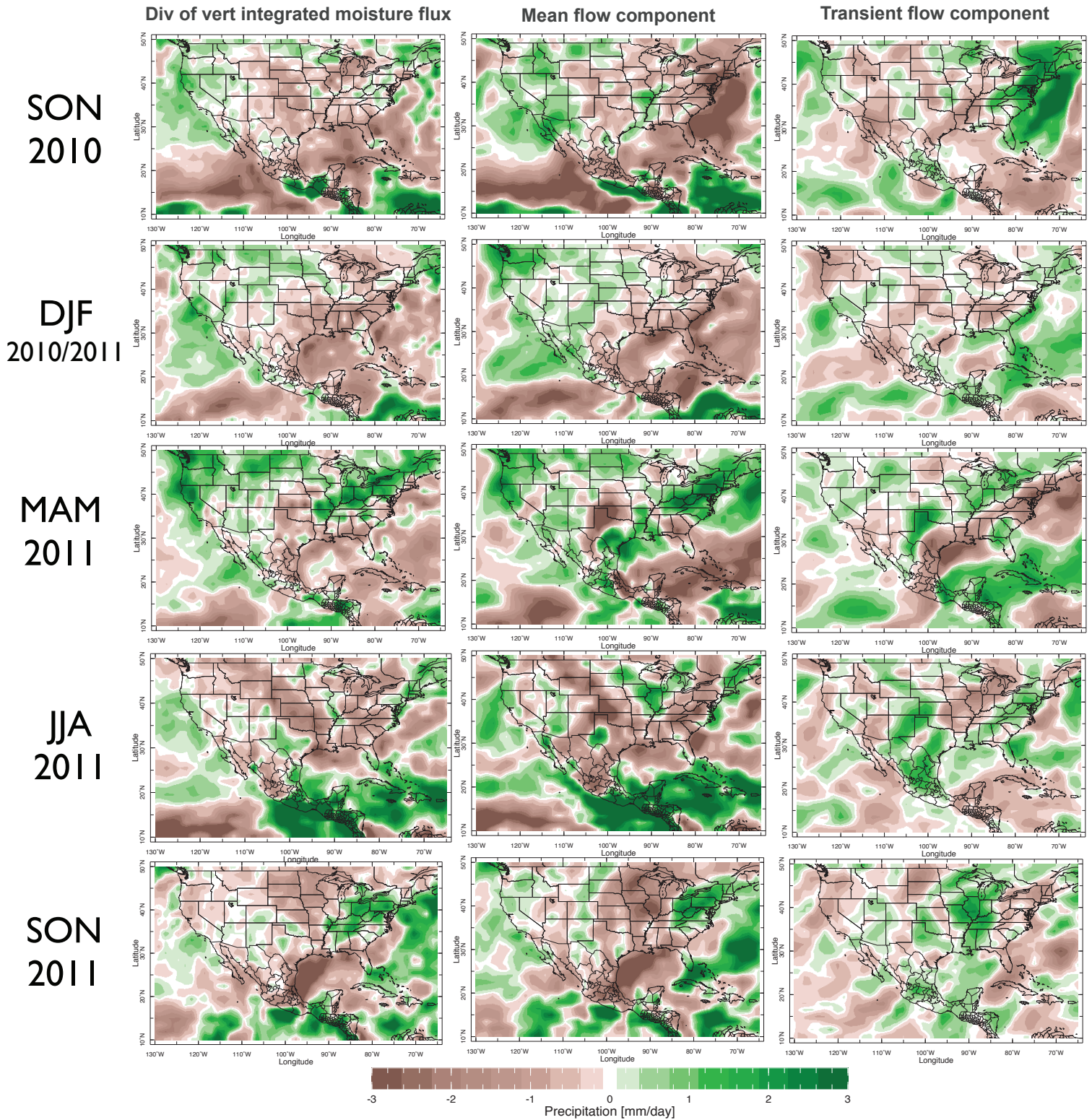


FIG. 12. Same as Figure 8 but using the ERA-Interim Reanalysis (relative to a 1979 to 2011 climatology). The monthly mean state and transient contributions are in the middle and right columns, respectively while the left column shows the anomalies in the convergence of the vertically integrated moisture transports as reported within the ERA-Interim data and which is well approximated by the sum of the two contributions.

Detrended 200 mb Height Anomaly

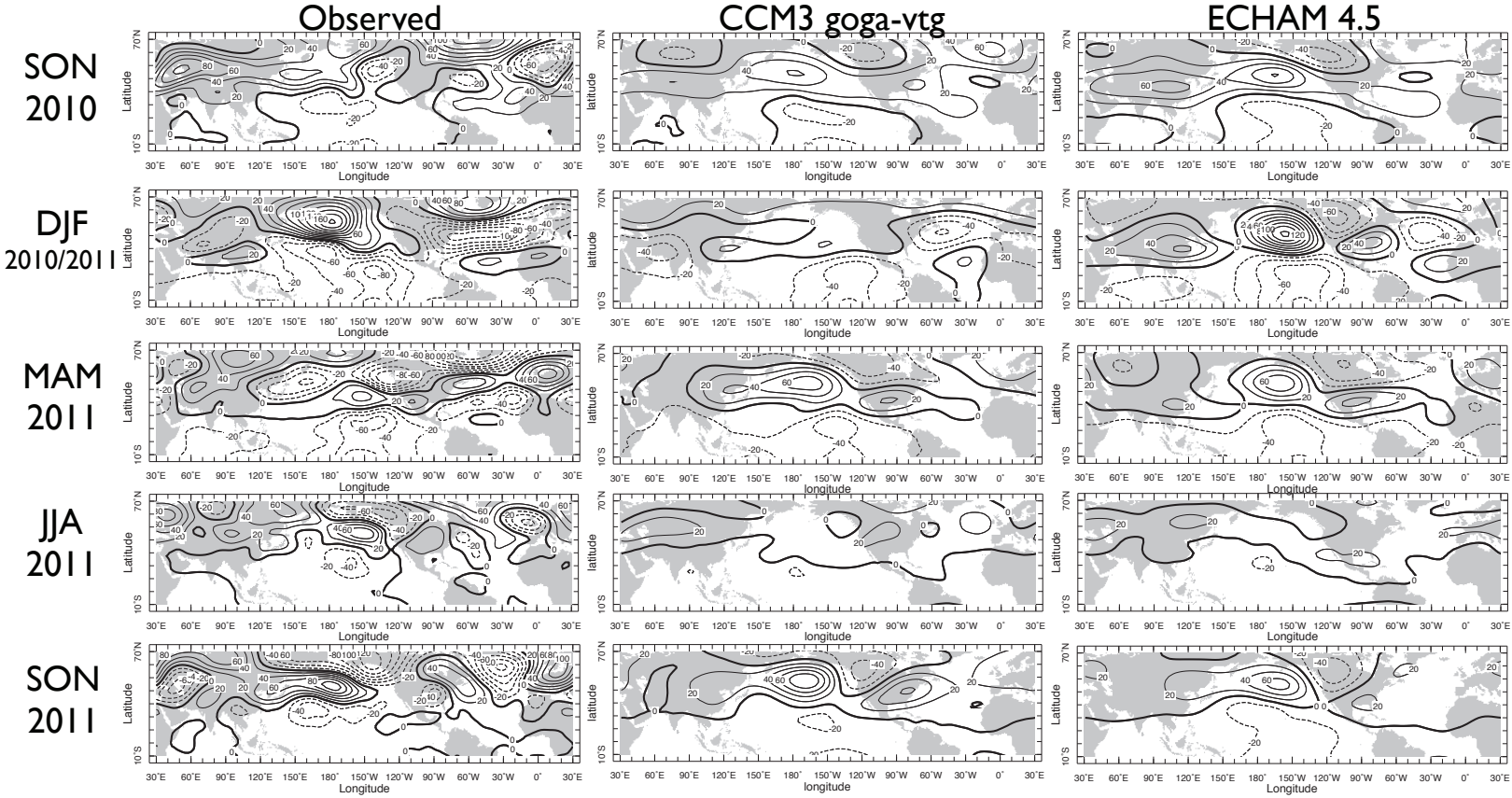


FIG. 13. The 200mb geopotential height anomalies for the seasons from SON 2010 to SON 2011 for the NCEP-NCAR Reanalysis (left), the CCM3 model (middle) and the ECHAM4.5 model (right). Heights were detrended to remove an overall increase caused by global warming. Units are meters.

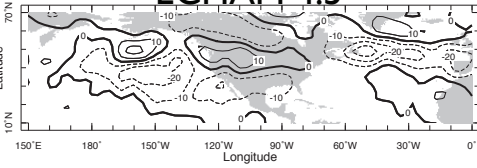
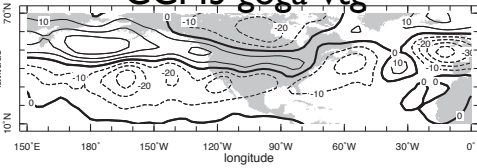
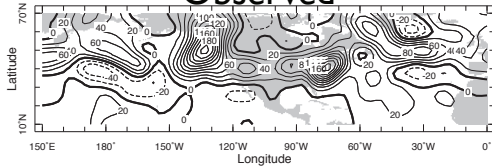
300 mb $\overline{v'^2}$ Anomaly

Observed

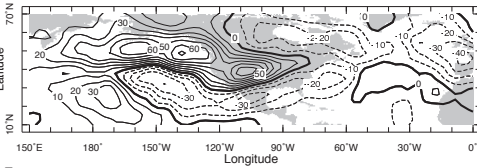
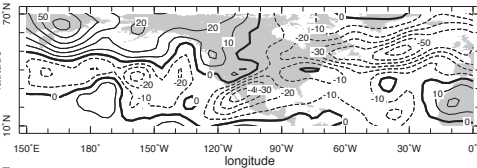
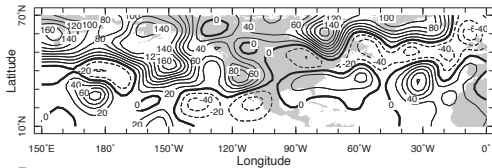
CCM3 goga-vtg

ECHAM 4.5

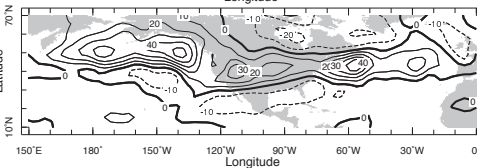
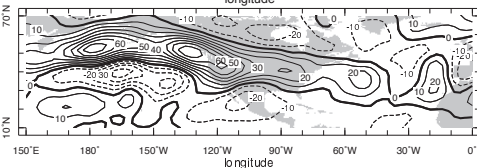
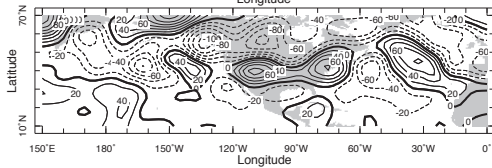
SON
2010



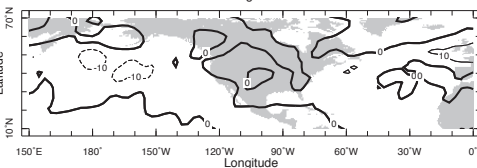
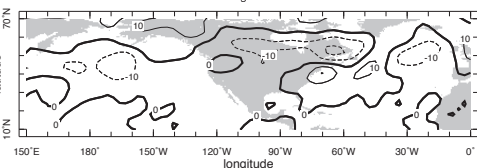
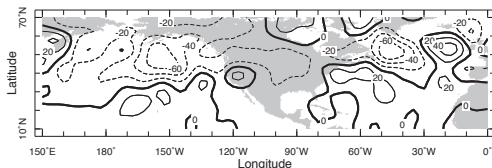
DJF
2010/2011



MAM
2011



JJA
2011



SON
2011

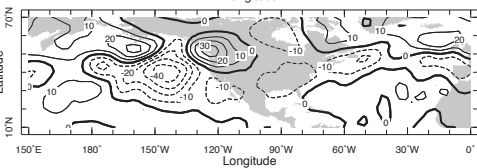
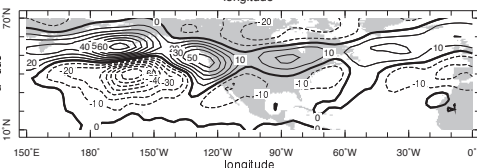
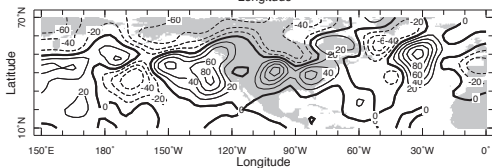


FIG. 14. Same as Figure 8 (with no detrending) but for the 300mb sub monthly eddy meridional velocity variance. Units are meters squared per second squared.

Precipitation vs. Surface Air Temperature JJA 1950–2011

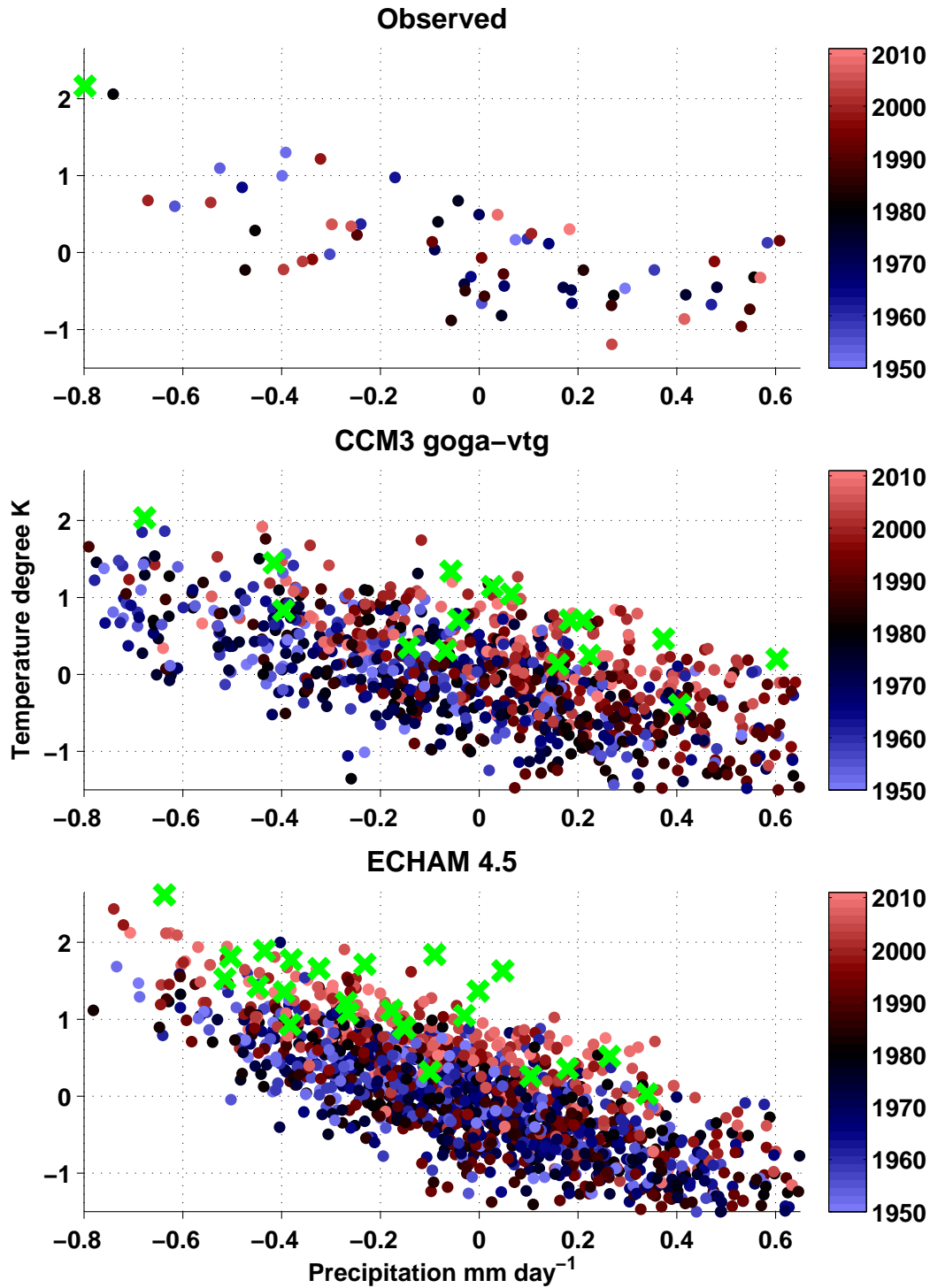


FIG. 15. Scatter plots of JJA temperature (Kelvin) and precipitation (mm/day) anomalies for the TexMex region and the 1950 to 2011 period for observations (top), the CCM3 model (middle) and the ECHAM4.5 model (bottom).

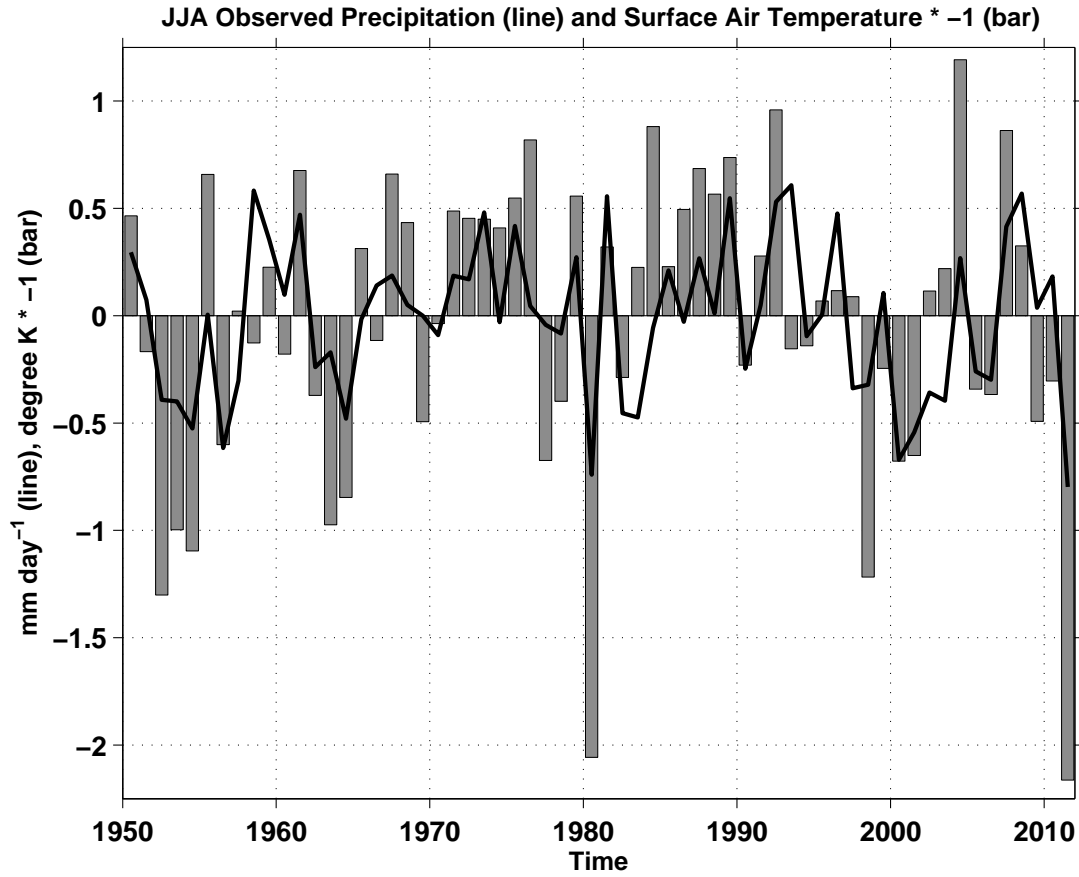


FIG. 16. Time history of observed JJA temperature (bars, Kelvin) and precipitation (line, mm/day) anomalies for the TexMex region and the 1950 to 2011 period.

IRI 4 Month Lead Forecasts

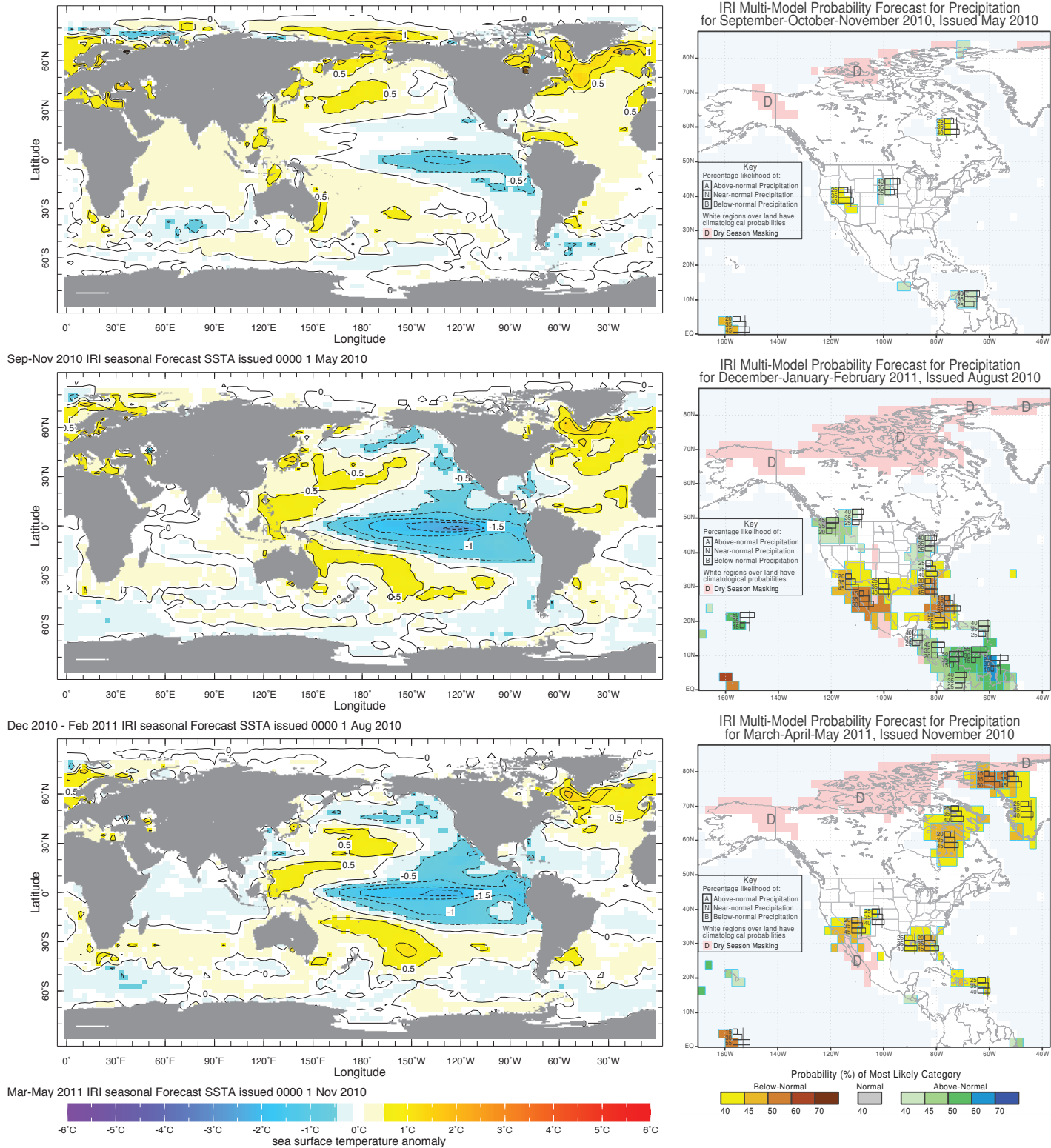


FIG. 17. The 4 month lead time forecasts of SSTA (left) and North American precipitation (right) from the IRI seasonal-to-interannual prediction system for SON 2010 from May 2010 (top), DJF 2010-11 from August 2010 (middle) and MAM 2011 from November 2010 (bottom).

IRI 4 Month Lead Forecasts

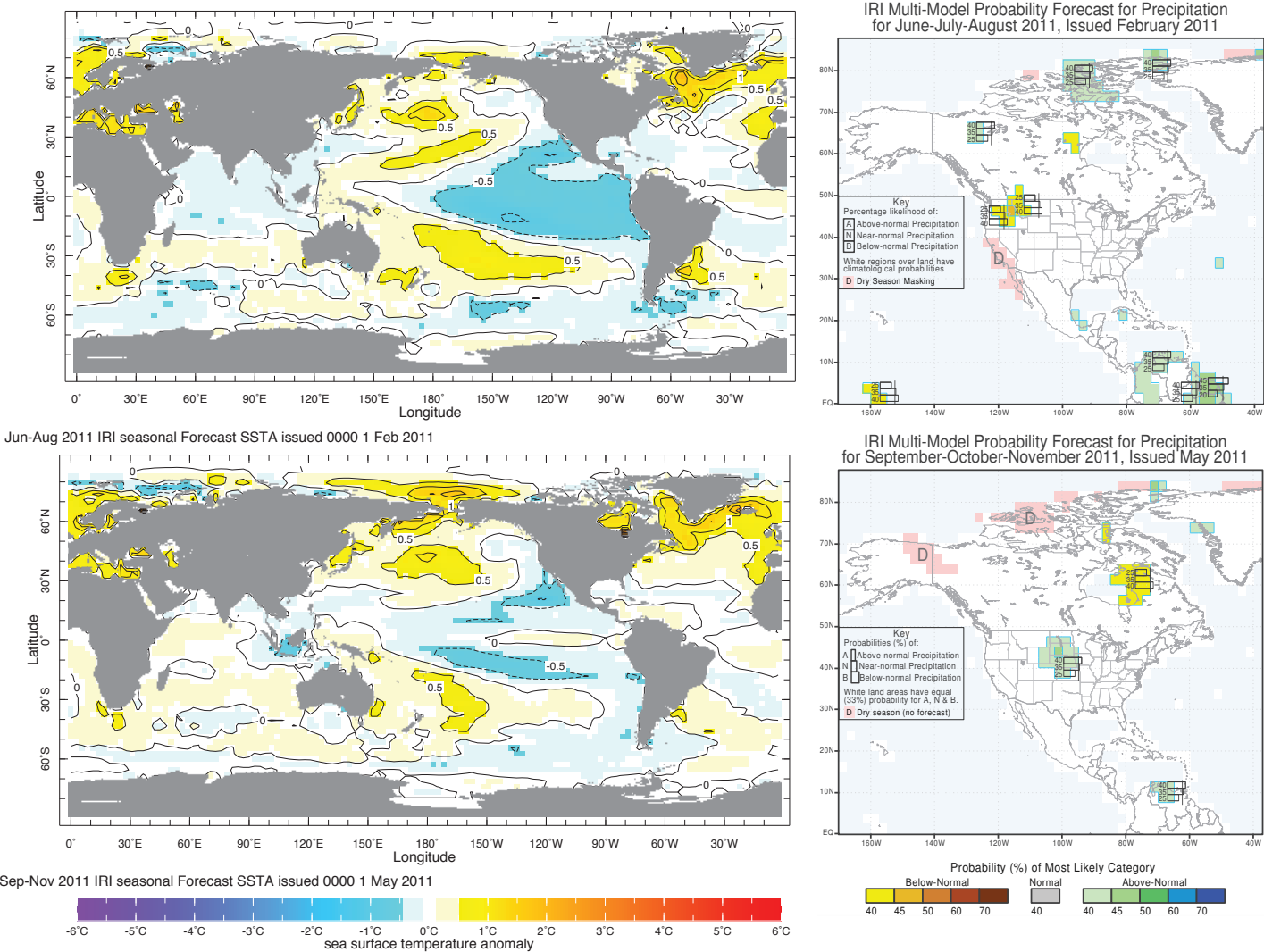


FIG. 18. Same as Figure 13 but for forecasts of JJA 2011 from February 2011 (top) and SON 2011 from May 2011 (bottom).